

1 **Responses of field-grown maize to different soil types, water regimes, and**
2 **contrasting vapor pressure deficit**

3 Thuy Huu Nguyen¹, Thomas Gaiser¹, Jan Vanderborght³, Andrea Schnepf³, Felix Bauer³, Anja
4 Klotzsche³, Lena Lärm³, Hubert Hüging¹, Frank Ewert^{1,2}

5 ¹University of Bonn, Institute of Crop Science and Resource Conservation (INRES), Katzenburgweg 5, 53115
6 Bonn, Germany

7 ²Leibniz Centre for Agricultural Landscape Research (ZALF), Institute of Landscape Systems Analysis,
8 Eberswalder Strasse 84, 15374 Muencheberg, Germany

9 ³Agrosphere (IBG-3), Institute of Bio- and Geosciences, Forschungszentrum Jülich GmbH, 52428, Jülich,
10 Germany

11 *[Corresponding author, email: tngu@uni-bonn.de](mailto:tngu@uni-bonn.de)

12 **Abstracts**

13 Drought is a serious constraint to crop growth and production of important staple crops such as maize.
14 Improved understanding of the responses of crops to drought can be incorporated into cropping system
15 models to support crop breeding, varietal selection and management decisions for minimizing negative
16 impacts. We investigate the impacts of different soil types (stony and silty) and water regimes (irrigated
17 and rainfed) on hydraulic linkages between soil and plant, as well as root: shoot growth characteristics.
18 Our analysis is based on a comprehensive dataset measured along the soil-plant-atmosphere pathway at
19 field scale in two growing seasons (2017, 2018) with contrasting climatic conditions (low and high VPD).
20 Roots were observed mostly in the topsoil (10-20 cm) of the stony soil while more roots were found in the
21 subsoil (60-80 cm) of the silty soil. The difference in root length was pronounced at silking and harvest
22 between the soil types. Total root length was 2.5 - 6 times higher in the silty soil compared to the stony

23 soil with the same water treatment. At silking time, the ratios of root length to shoot biomass in the rainfed
24 plot of the silty soil (F2P2) were 3 times higher than those in the irrigated silty soil (F2P3) while the ratio
25 was similar for two water treatments in the stony soil. With the same water treatment, the ratios of root
26 length to shoot biomass of silty soil was higher than stony soil. The observed minimum leaf water potential
27 (ψ_{leaf}) varied from around -1.5 MPa in the rainfed plot in 2017 to around -2.5 MPa in the same plot of the
28 stony soil in 2018. In the rainfed plot, the minimum ψ_{leaf} in the stony soil was lower than in silty soil from
29 -2 to -1.5 MPa in 2017, respectively while these were from -2.5 to -2 MPa in 2018, respectively. Leaf water
30 potential, water potential gradients from soil to plant roots, plant hydraulic conductance (K_{soil_plant}),
31 stomatal conductance, transpiration, and photosynthesis were considerably modulated by the soil water
32 content and the conductivity of the rhizosphere. When the stony soil and silt soil are compared, the higher
33 'stress' due to the lower water availability in the stony soil resulted in less roots with a higher root tissue
34 conductance in the soil with more stress. When comparing the rainfed with the irrigated plot in the silty
35 soil, the higher stress in the rainfed soil resulted in more roots with a lower root tissue conductance in the
36 treatment with more stress. This illustrates that the 'response' to stress can be completely opposite
37 depending on conditions or treatments that lead to the differences in stress that are compared. To respond
38 to water deficit, maize had higher water uptake rate per unit root length and higher root segment
39 conductance in the stony soil than in the silty soil, while the crop reduced transpired water via reduced
40 aboveground plant size. Future improvements of soil-crop models in simulating gas exchange and crop
41 growth should further emphasize the role of soil textures on stomatal function, dynamic root growth, and
42 plant hydraulic system together with aboveground leaf area adjustments.

43 **Key words:** irrigation, plant hydraulic conductance, transpiration, root length, soil types, soil to leaf water
44 potential, stomatal regulation

45 **Abbreviations:** DOY: day of the year; DAS: day after sowing; TUE: transpiration use efficiency; SF: sap flow;
46 LAI: green leaf area index; PAR: photosynthetically active radiation; VPD: vapor pressure deficit; An: net

47 leaf photosynthesis; E: leaf transpiration; ψ_{leaf} : leaf water potential; $\psi_{\text{sunlitleaf}}$: leaf water potential of sunlit
48 leaf; $\psi_{\text{shadedleaf}}$: leaf water potential of shaded leaf; K_{soil} : hydraulic conductance of soil; K_{root} : root hydraulic
49 conductance; K_{stem} : stem hydraulic conductance; $\psi_{\text{soil_effec}}$: effective soil water potential; $\psi_{\text{difference}}$:
50 difference between effective soil water potential and sunlit leaf water potential; $K_{\text{soil_root}}$: root system
51 hydraulic conductance (includes soil and root hydraulic conductance); $K_{\text{soil_plant}}$: whole plant hydraulic
52 conductance (includes below and aboveground components).

53 **1. Introduction**

54 Maize (*Zea mays L.*) is a major staple crop throughout the world. Drought stress, which negatively affects
55 crop growth and yield, is of increasing concern in several important maize cultivating regions (Daryanto et
56 al., 2016). Increases in frequency and severity of drought events due to climate change have been recently
57 reported (IPCC, 2022). Thus, field observations and understanding on how maize responds to water stress
58 are necessary to suggest promising traits for breeding programs (Vadez et al., 2021) as well as irrigation
59 schemes (Fang and Su, 2019; Q. Cai et al., 2017). Improved understanding of crops' response to drought
60 can be incorporated into soil-crop models (e.g. crop modelling and soil-vegetation-atmosphere transfer
61 modelling).

62 Stomatal regulation is often considered as a key aboveground hydraulic variable in regulating water use
63 of crops. Maize was considered as isohydric plant in which stomata are closed in response to sensing
64 drought conditions to maintain leaf water potential (ψ_{leaf}) above critical levels ($\psi_{\text{threshold}}$ or minimum ψ_{leaf})
65 (Tardieu and Simonneau, 1998). Investigations of how stomatal controls differ among species and
66 genotypes commonly observed minimum ψ_{leaf} or analyzed **ef** genetic variability of stomatal control in
67 response to varying soil water content. Analyzing measurements of ψ_{leaf} from 400 lines of maize of tropical
68 and European origins under greenhouse and growth chamber conditions, Welcker et al. (2011) reported
69 values of minimum ψ_{leaf} from -0.8 to -1.5 MPa, indicating genetic variability of stomatal responses. The
70 isohydric behavior is due to different mechanisms including hydraulic and/or chemical (e.g. abscisic acid

71 [ABA] signals (Tardieu, 2016). The degree to which these underlying mechanisms interact and differ
72 among genotypes and/or environmental scenarios in explaining the stomatal regulation is still debated
73 (Tardieu, 2016, Hochberg et al., 2018). Field evidence in variation of the minimum ψ_{leaf} of maize due to soil
74 water availability is rarely reported.

75 Water flow along the soil-plant-atmosphere continuum is determined by a series of hydraulic
76 conductivities and gradients in water potential. Hydraulic conductance of soil (K_{soil}), root hydraulic
77 conductance (K_{root}), and stem hydraulic conductance (K_{stem}) determine water potential from soil to root
78 and root xylem water, and thus magnitude of ψ_{leaf} . There are two main resistances to water flow from the
79 soil to the shoot, namely the soil and the root resistances, often expressed as their inverse, K_{soil} and K_{root}
80 (Nguyen et al., 2020; Cai et al., 2018). In wet soils, the soil hydraulic conductivity is much higher than that
81 of roots, and water flow is mainly controlled by root hydraulic conductivity (Hopmans and Bristow, 2002;
82 Draye et al., 2010). It is well-known that a decrease in soil matric potential and soil hydraulic conductivity
83 triggers stomatal closure and thus results in reduction in transpiration rate (Sinclair and Ludlow, 1986;
84 Carminati and Javaux 2020; Abdalla et al., 2021). For the root water uptake and controlling stomata, the
85 location where soil and roots are in close contact (rhizosphere) is most important, because when this thin
86 layer of rhizosphere is disconnected (i.e. soil-root contact is lost), the water movement from soil toward
87 the roots is reduced, which might trigger stomatal closure to maintain hydraulic integrity of plant
88 (Carminati et al., 2016; Rodriguez-Dominguez and Brodribb, 2019; Abdalla et al., 2022). The magnitude of
89 the drop of water potential between bulk soil and soil-root interface increases considerably at different
90 levels of soil dryness for different soil types (Carminati and Javaux, 2020; Abdalla et al., 2022). Hydraulic
91 limits in the soil (Carminati and Javaux, 2020), or in the root-soil interface [as measured for olive trees by
92 Rodriguez-Dominguez and Brodribb, 2019 or tomato (Abdalla et al., 2022)], or in the root properties
93 (Bourbia et al., 2021; Cai et al., 2022; Nguyen et al., 2020; Cai et al., 2018) or due to both soil textures and
94 root phenotypes (Cai et al., 2022b) emphasized the importance of belowground hydraulics (Carminati and

95 Javaux, 2020). However, also the shoot hydraulic conductance could be limiting in some crop plants
96 (Gallardo et al., 1996) or in trees (Domec and Pruyn, 2008; Tsuda and Tyree, 1997). Stomatal conductance
97 and shoot hydraulic conductance showed close links to each other in pine trees (Hubbard et al., 2001).
98 This summary illustrates three points: (i) current studies have often focused either on above or on below
99 hydraulic limits, but rarely consider both (ii) it is unclear the roles and relations of soil hydraulic properties
100 to root and plant hydraulic conductance (thus influences on stomatal conductance) (iii) the role of different
101 hydraulic processes across the soil - plant - atmosphere continuum i.e. soil to roots, stem, and soil-plant
102 hydraulic conductance in controlling stomatal conductance remains unclear.

103 Simultaneous measurements of atmospheric conditions (light intensity and vapor pressure deficit), leaf
104 water potential, and transpiration rates, coupled with measurements of root, stem and whole soil-plant
105 hydraulic conductance, root architecture, and soil water potential distribution could reveal the relative
106 importance of rhizosphere, shoot and root growth, and hydraulic conductance vulnerability, especially
107 under progressive soil drying at field conditions (Carminati and Javaux, 2020; Tardieu et al., 2017). For the
108 soil water conditions, soil texture and hydraulic characteristics are very important ~~that-because they~~
109 influence soil water movement and thus affect infiltration, surface and sub-surface runoff, and ultimately
110 plant available soil water (Vereecken et al., 2016). Soil texture properties, characterized by different
111 fractions of clay, silt, and sand particles, are important drivers in determining the soil water retention
112 properties (Scharwies and Dinneny, 2019; Stadler et al., 2015; Zhuang et al., 2001). Soil with higher water
113 holding capacity (here the silty soil with low stone content) have a larger amount of plant available water
114 which in turn enables crops to better meet the evaporative demand and facilitates better crop growth as
115 compared to the soil with high stone content (Nguyen et al., 2020; Cai et al., 2018). Estimations of hydraulic
116 conductance (different organs and whole plant hydraulic conductance) were done for crop plants and
117 maize mainly under controlled environment or pot conditions e.g. for different species and genotypes
118 during soil drying (Sunita et al., 2014; Choudhary and Sinclair, 2014; Abdalla et al., 2022; Meunier et al.,

119 2018; Wang et al., 2017; Li et al., 2016) or various species and genotypes together with different soil
120 textures (Cai et al., 2022a), or soil texture with different vapor pressure deficit (VPD) (Cai et al., 2022b).
121 Compared to the substantial effect of soil texture, there was no evidence of an effect of VPD on both soil–
122 plant hydraulic conductance and on the relation between canopy stomatal conductance and soil–plant
123 hydraulic conductance in pot-grown maize (Cai et al., 2022b). Contrast results were found in winter wheat
124 where plant hydraulic conductance increased with rising VPD for some genotypes in wet conditions
125 (Ranawana et al., 2021). Vadez et al., (2021) examined the effects of soil types together with increasing
126 VPD on transpiration efficiency (TE) and yield under pot conditions for several C₄ species (maize, sorghum,
127 and millet). The interpretation of differences in TE was attributed to soil types, more specifically, to the
128 differences in soil hydraulic properties and soil hydraulic conductance. However, experimental evidence
129 linking root hydraulics to stomatal regulation was lacking in these two Vadez’s studies (Vadez et al., 2021).
130 Extrapolation and use of results obtained in pots or under greenhouse conditions to the field scale are
131 difficult due to the fact that soil substrates in pots might not represent natural soil in the field (Passioura,
132 2006). There is often greater evaporative demand and considerable fluctuation and interactions of climatic
133 variables in the field as compared to experiments under controlled or semi-controlled conditions. Recent
134 field studies have aimed at quantification of root hydraulic conductance and it’s linkages with crop growth
135 (leaf area and biomass) under different soil types (in wheat Cai et al., 2017; Cai et al., 2018; Nguyen et al.,
136 2020 or maize in Nguyen et al., 2022; Jorda et al., 2022). However, field studies that consider both below
137 (soil-root hydraulic conductance) and above (stem hydraulic conductance), or soil-plant hydraulic
138 conductance (including below and above-ground parts) and their roles in stomatal regulation as well as
139 crop growth (leaf area and biomass) are rarely carried out.

140 This study aims at further understanding of the hydraulic linkages between soil and plant and responses
141 of plants to drought stress in relation to root: shoot growth characteristics at field scale. We hypothesize
142 that, in field-grown maize, (1) soil-plant hydraulic conductance depends on soil hydraulic properties,

143 especially under dry soil conditions (2) minimum leaf water potential of maize is similar across soil types,
144 water treatments and climatic conditions. The hypotheses will be tested through three objectives: (i) to
145 investigate the effects of soil types, water application, and climatic condition on root growth and (ii) on
146 stomatal conductance, leaf photosynthesis, transpiration, leaf water potential, different components
147 ~~(root, stem and whole soil-plant of-the~~ hydraulic conductance (root, stem, and whole soil-plant), and (iii)
148 to analyze the relative contribution of root and shoot growth (leaf area and biomass) on the water uptake
149 capacity of maize. These three objectives will be achieved based on a comprehensive dataset covering the
150 whole soil-plant continuum over two growing maize seasons with contrasting climatic conditions (low and
151 high VPD) under two water treatments (rainfed and irrigated) and two different soil types (stony and silty
152 soil).

153 **2. Materials and methods**

154 **2.1. Location and experimental set-up**

155 We carried out a field experiment at two rhizotron facilities in Selhausen, North Rhine-Westphalia,
156 Germany (50°52'N, 6°27'E). The field is slightly inclined with a maximum slope of around 4°. One rhizotrone
157 facility was located upslope (F1) with around 60% gravel by weight in the 10-cm topsoil while the second
158 rhizotrone facility was at downslope (F2) with silty soil (stone content is around 4% by weight).

159 Each ~~experimental site~~ rhizotrone facility was divided into three subplots of 7.25 m by 3.25 m: two rainfed
160 plots (P1, P2), and one irrigated plot (P3). In rainfed plots P1, other sowing densities and dates were used
161 than in the other plots and we excluded therefore these plots. Silage maize cv. Zoey was sown on 4 May
162 and 8 May in 2017 and 2018, respectively, with a plant density of 10.66 seeds m⁻² (Figure 1a; Table 1).
163 Detailed information of crop management practices is provided in Table 1.

164 [Insert Table 1 here]

165 **2.2. Water applications**

166 Weather variables (global radiation, temperature, relative humidity, precipitation, and wind speed) were
167 recorded every 10 minutes by a nearby weather station (approx. 100 m from the experiment). Drip lines
168 (T-Tape 520-20-500, Wurzelwasser GbR, Müzenberg, Germany) were installed for irrigation at 0.3 m
169 intervals parallel to the crop rows. In 2017, maize received a total amount of 230 mm precipitation during
170 the growing period (136 days). Average, minimum and maximum daily air temperature were 17.6, 8.3, and
171 25.3 °C, respectively (Fig. 1b). The crop on P3 was irrigated (in total 130 mm) every 5-7 days (in total 10
172 times) using 13 mm of irrigation water per event between mid June to end of August for the irrigated plots
173 (2017F1P3 and 2017F2P3) (Fig. 1b). In 2018, average, minimum, and maximum daily air temperature were
174 19.2, 10.85, and 27.3 °C, respectively (Fig. 1b) and exceeded those of 2017. Characterized by exceptionally
175 hot and dry weather conditions, the summer season 2018 can be classified as an extreme year with respect
176 to plant growth at our [experimental location site](#). Maize experienced high temperatures and VPD,
177 especially around tasseling and silking. In 2018, only 91.3 mm of rain were recorded in the growing period
178 of 2018 (107 days). The maize crop was irrigated every 5-7 days (in total 13 times), with a total amount of
179 irrigation of 257 mm and 239 mm between mid- June and mid- August for the irrigated plots 2018F1P3
180 and ~~2018F1P3~~2018F2P3, respectively (Fig. 1d). In contrast to 2017, the rainfed plot in the stony soil
181 (2018F1P2) had to be irrigated (in total 66 mm) ~~in~~ four times (using 13, 22, 13, and 18 mm, respectively)
182 to avoid a crop failure due to severe drought (Fig. 1d).

183 [Insert Figure 1 here]

184 **2.3. Measurements**

185 **2.3.1. Soil water measurement and root growth**

186 At soil depths of 10, 20, 40, 60, 80, and 120 cm, MPS-2 matrix water potential and temperature sensors
187 (Decagon Devices Inc., UMS GmbH München, Germany) were installed to measure half-hourly soil water
188 potential and soil temperature. The range of the water potential measurements is ~~from~~ from -9 kPa to

189 approximately -100000 kPa (pF 1.96 to pF 6.01). In addition to MPS-2, soil water potential was measured
190 by pressure transducer tensiometers (T4e, UMS GmbH, München, Germany) where the minimum
191 detectable suction is -85 kPa to +100 kPa. A detailed description of sensor installation, calibration and data
192 post processing can be found in Cai et al., (2016).

193 Minirhizotubes (7 m long clear acrylic glass tubes with outer and inner diameters of 6.4 and 5.6 cm,
194 respectively) were installed horizontally at six different depths of 10, 20, 40, 60, 80, and 120 cm below the
195 soil surface in each facility. There are three replicate tubes at each depth, accounting for 54 tubes in each
196 facility. Root measurements were taken manually by Bartz camera (Bartz Technology Corporation) (23
197 June 2017 – 12 September 2017) and VSI camera (Vienna Scientific Instruments GmbH) (08 June 2017 – 22
198 June 2017) in 2017 while only VSI was used in 2018 (23 May 2018 - 23 August 2018). Root images were
199 taken at 20 fixed positions from the left- and right-hand sides of each tube weekly (or biweekly) during the
200 growing seasons~~Root images were repeatedly taken from both left and right sides at 20 locations along~~
201 ~~horizontally installed minirhizotubes.~~ The root images were analyzed by automated minirhizotube image
202 analysis pipeline for segmentation and automated feature extraction (Bauer et al., 2021). Two-dimensional
203 root length density (RLD, in units of cm cm^{-2}) was estimated from the total root length observed in the
204 image and the image surface area. The overview of camera system, minirhizotube images acquisition, and
205 post-processing of the root data were described in detail in Bauer et al. (2021) and Lärm et al., (2023).

206 **2.3.2. Crop growth measurement**

207 The phenology, plant height, stem diameter, green and brown leaf area, dry matter of different organs,
208 and total aboveground dry matter were observed and measured bi-weekly. Plant height was measured
209 ~~ein~~ 15 randomly selected plants. The diameters of five randomly selected stems were measured. Due to
210 the limited number of plants in each plot, only two plants per measurement date were sampled to
211 determine total aboveground dry matter and leaf area (7 and 8 times in 2017 and 2018, respectively).

212 Green and brown leaf area was measured by a LI-3100C (Licor Biosciences, Lincoln, Nebraska, USA). At
213 harvest, five separate replicates (1m² each) were harvested. The dry matter of separate organs was
214 determined after drying at 105 °C for 48 hours (Nguyen et al., 2020).

215 **2.3.3. Leaf gas exchange, leaf water potential, and sap flow measurements**

216 Hourly leaf stomatal conductance (Gs), net photosynthesis (An), and leaf transpiration (E) were measured
217 every two weeks under clear sky conditions. Observations from 8 AM to 5 PM on four days and from 10
218 AM to 4 PM on six days were carried out in 2017. In 2018, measurements were carried out on 6 days from
219 8 AM to 7 PM and on 5 days from 10 AM to 4 PM (Nguyen et al., 2022a). The Gs, An, and E of two sunlit
220 leaves (uppermost fully developed leaves) and one shaded leaf of different plants were measured at
221 steady-state using a LICOR 6400 XT device (Licor Biosciences, Lincoln, Nebraska, USA). After leaf gas
222 exchange measurements, leaves were quickly detached using a sharp knife to measure leaf water potential
223 (ψ_{leaf}) with a digital pressure chamber (SKPM 140/ (40-50-80), Skye Instrument Ltd, UK) with the working
224 air pressure ranging from 0 to 35 bars. To study the diurnal course of ψ_{leaf} under dry and re-wetted soil
225 conditions, in 2018, measurements were undertaken for three additional days with predawn
226 measurements two days before and one day after irrigation. Further detail of measurement dates, range
227 of real time records of PAR, VPD and soil water status could be found in (Nguyen et al., 2022a).

228 In 2017 (from 7 July 2017 until harvest) and 2018 (from 28 June 2018 until harvest), 20 sap flow sensors
229 (SGA 13, SGB 16, and SGB 19 types) were installed (one sensor per plant and 5 maize plants per plot) based
230 on stem diameter size. Sensor data, in particular the partitioning of energy, electricity supply, sap flow,
231 and the temperature difference between upper and lower thermocouples (dT) of each sensor were
232 recorded at 10 minute intervals using a CR1000 data logger and two AM 16/32 multiplexers (Campbell
233 Scientific, Logan, Utah). The sap flow in the plant (g h^{-1}) was monitored directly by the data loggers

234 (Dynamax, 2007) and used as a surrogate for canopy transpiration based on the number of plants per
235 square meter.

236 **2.4. Calculation of total root length, root system conductance, stem, and whole plant hydraulic** 237 **conductance**

238 To estimate the total root length from minirhizotubes, we adopted the option 2 which was described in
239 Cai et al., (2017). Total root length per square meter soil surface area within each soil layer ($m\ m^{-2}$) was
240 computed by multiplying the root length density with the corresponding soil layer thickness. The root
241 length density was determined in each depth by dividing the measured root length per minirhizotron
242 image by the assumed volume the roots would have occupied in absence of the tube, i.e., $W * L * \text{tube}$
243 radius (see Cai et al., 2017).

244 Following Nguyen et al., (2020), the effective soil water potential was calculated based on hourly measured
245 soil water potential (ψ_i) and normalized root length density at six depths (10, 20, 40, 60, 80, and 120 cm)
246 (NRLD_i), and soil layer thickness (Δz_i) in the soil profile (Equation 1).

$$\psi_{soil_effec} = \sum_{i=1}^N \psi_i NRLD_i \Delta z_i \quad (1)$$

247 We followed Ohm's law analogy by dividing the hourly sap flow by the difference between effective soil
248 water potential and shaded leaf water potential to estimate root system conductance (K_{soil_root} - Equation
249 2), between shaded leaf water potential and sunlit leaf water potential to estimate stem hydraulic
250 conductance (K_{stem} - Equation 3), and between effective soil water potential and sunlit leaf water potential
251 to estimate whole plant hydraulic conductance (K_{soil_plant} - Equation 4).

$$K_{soil_root} = Sapflow / (\psi_{soil_effec} - \psi_{shadedleaf}) \quad (2)$$

$$K_{stem} = Sapflow / (\psi_{shadedleaf} - \psi_{sunlitleaf}) \quad (3)$$

$$K_{soil_plant} = Sapflow / (\psi_{soil_effec} - \psi_{sunlitleaf}) \quad (4)$$

252 During one measurement day, four values of the K_{soil_root} , K_{stem} , and K_{soil_plant} were obtained from
253 measurements between 11AM and 2 PM. The average and standard deviation of these hourly
254 measurements were calculated for each measurement day in order to present the seasonal dynamics of
255 those variables. To capture the diurnal and seasonal variations of sap flow and sunlit leaf water potential,
256 in addition, we plotted the hourly sap flow and hourly difference of effective soil water potential and sunlit
257 leaf water potential for three measurement days starting from predawn and whole seasons, respectively,
258 to derive the slope which is also K_{soil_plant} .

259 2.5. Statistical analysis

260
261 Regression analysis was performed to understand the relationship between the sap flow volume and the
262 difference of effective soil water potential and sunlit leaf water potential as well as the relationship
263 between the total aboveground biomass and cumulated water transpired (sap flow volume). These
264 analyses allow to derive the slope as proxy of K_{soil_plant} and transpiration use efficiency, respectively. Since
265 all measured data have their own measurement errors, the generalized Deming regression was employed.
266 We performed relationships (via correlation coefficient and statistical significant levels) of midday leaf A_n ,
267 G_s , and E with midday K_{stem} , K_{soil_plant} , K_{soil_root} , sunlit leaf potential, ψ_{soil_effec} , and the difference of ψ_{soil_effec}
268 and sunlit leaf water potential ($\psi_{difference}$). All data processing and analysis were conducted using the R
269 statistical software (R Core Team, 2022).

270 3. Results

271 3.1. Root growth under different water treatments, soil types and climatic conditions

272 Observed root length ($cm\ cm^{-2}$) from the minirhizotubes in different soil depths at the first week of June
273 (stem elongation), around silking, and at harvest in two growing seasons are shown in the Figure 2. Root
274 length was similar among water treatments at the start of stem elongation in both years (Fig. 2a & 2d).

275 The difference in root length was pronounced at silking and harvest between the soil types. More root
276 growth was observed in the silty soil compared to the stony soil with the same water treatment (i.e. 2.5 -
277 6 times higher at depth 40 cm). This indicated the strong negative effects of stone content on root
278 development. In the stony soil, root length in the irrigated plot (F1P3) was slightly higher than in the rainfed
279 plot (F1P2). In contrast, the rainfed treatment (F2P2) in the silty soil showed much higher root length,
280 especially from 40 to 120 cm depths as compared to the irrigated plot (F2P3) in both growing seasons.
281 Much lower stone content and deep soil cracks in the silty soil (Morandage et al., 2021) allow root
282 extension to the subsoil, particularly in the rainfed plot F2P2. Root length in the rainfed treatment (F2P2)
283 in 2018, is higher than in 2017 which implies that root further developed to exploit the water in the soil
284 under the rainfed condition to meet the higher evaporative demand.

285 [Insert Figure 2 here]

286 Total root length (m m^{-2}) estimated from minirhizotubes and its ratio to shoot dry matter (m kg^{-1}) at three
287 measured dates (as in Figure 2) are shown in the Figure 3. Total root length was much higher for the silty
288 plots as compared to stony plots. In 2017, the highest total root length was observed in the rainfed plot of
289 the silty soil (F2P2) with approximately 9166 m m^{-2} and 9878 m m^{-2} around silking and harvest, respectively,
290 which was almost two times higher than in the irrigated plot (F2P3). These figures were higher in 2018
291 than 2017 where total root length of F2P2 was 10188 m m^{-2} and 13750 m m^{-2} at silking and harvest time,
292 respectively. For the rainfed stony soil (F1P2), soil water depletion around the beginning of June in 2017
293 (Supplementary material 1a) and from the first two weeks of June to harvest in 2018 (Supplementary
294 material 2a) caused the strong reduction of shoot biomass. In the stony soil, the shoot dry matter of the
295 irrigated plot (F1P3) and the rainfed plot (F1P2) were 1275 and 536 g m^{-2} at silking time (e.g. 19 July 2018
296 –DOY 200, Supplementary material 3a and 3b). However, there was a minor difference between F1P2 and
297 F1P3 in terms of the ratio of root length to shoot dry matter. In the silty soil, a decrease of soil water
298 potential was not pronounced (compared to stony soil) in both years 2017 and 2018 (Supplementary

299 material 1b and 2b). In 2018, shoot biomass in the irrigated stony soil (F1P3) and silt soil (F2P3) were
300 similar (1275 and 1299 g m⁻², respectively on 19 July 2018 – DOY 200) while the shoot biomass of the
301 rainfed silty soil (F2P2) was 876 g m⁻² (Supplementary material 3a & 3b). However, the ratios of root length
302 to shoot biomass in the rainfed plot of the silty soil (F2P2) were 3 and 6 times higher than those in the
303 irrigated silty soil (F2P3) and stony soil (F1P3), respectively (e.g. 18 July, DOY 199). Moreover, total root
304 length was relatively equal among treatments at the start of set elongation (8 June - DOY 159, ~~first week~~
305 ~~of June~~) in both years, while this was the opposite for the ratio of root length to shoot dry matter. This
306 firstly illustrated that the finer soil texture without stones and with soil cracks could favor the root growth
307 which indicates strong interactions of root and soil conditions. Secondly, the larger root length and higher
308 atmospheric evaporative demand in 2018 than 2017 indicates also the interaction of root growth and
309 climatic conditions.

310 [Insert Figure 3 here]

311 **3.2. Stomatal conductance, photosynthesis, transpiration, and K_{soil_plant}**

312 **3.2.1. Diurnal course of stomatal conductance, photosynthesis, transpiration, and water potential at leaf** 313 **level**

314 After a long period with high temperatures and no rainfall, soil water reduction in the rainfed plot of the
315 stony soil (F1P2) on 17 July 2018 (Supplementary material 2) resulted in three times lower net
316 photosynthesis (A_n), stomatal conductance (G_s), transpiration (E) and leaf water potential (ψ_{leaf}) as
317 compared to the remaining treatments (Fig. 4). This indicates that the soil water content strongly affected
318 the stomatal conductance. Stomatal closure was much pronounced around midday in F1P2 while this was
319 not the case in the F2P2, indicating the soil type strongly affected the stomatal conductance and leaf gas
320 exchange.

321 [Insert Figure 4 here]

322 Leaf gas exchange and leaf water potential in the F1P2 were still much lower than in other plots (Figure
323 5). On 18 July 2018, after application of 22.75 mm of irrigation water (at 4 PM), photosynthesis, stomatal
324 conductance, transpiration and leaf water potential were slightly increased in F1P2. However, these were
325 still smaller than in F2P2 and the two irrigated plots.

326 [Insert Figure 5 here]

327 On the next day after irrigation, leaf gas exchange and water potential were considerably increased in the
328 F1P2 (Figure 6). Leaf curling was also less pronounced as compared the two previous days. This indicated
329 the recovery of plant after watering. Leaf water potential, photosynthesis, stomatal conductance, and leaf
330 transpiration were almost similar to other plots from predawn throughout the day.

331 [Insert Figure 6 here]

332 **3.2.2. Seasonal course of stomatal conductance, photosynthesis, transpiration, water potential, and** 333 **plant hydraulic conductance at the leaf level**

334 Seasonal stomatal conductance (G_s) and leaf water potential (ψ_{leaf}) are described in Figure 7. The
335 relationship between two variables was rather noisy and non-linear. The leaf water potential showed
336 distinct patterns among treatments in one growing season. Minimum ψ_{leaf} was maintained at around -1.5
337 MPa in the irrigated plot in stony soil (F1P3) and two plots in the silty soil (F2P2 and F2P3). Lower minimum
338 ψ_{leaf} could be observed in the rainfed plot with stony soil (F1P2) but it did not go beyond -2 MPa. Minor
339 leaf curling was observed only in the second week of June in the F1P2 in 2017. In 2018, the higher
340 temperature and vapor pressure deficit resulted in lower minimum ψ_{leaf} in all treatments and soil types as
341 compared to 2017. The minimum ψ_{leaf} was around -2 MPa in F1P3, F2P2, and F2P3 while ψ_{leaf} could drop
342 below -2 MPa in F1P2 which was due to the severe soil water deficit. The low G_s and ψ_{leaf} associated with
343 measurement dates when the substantial leaf curling was observed at mid of July to the end of growing
344 season in F1P2 in 2018 (Supplementary material 3c & 3d and Supplementary material 4c & d).

345 [Insert Figure 7 here]

346 The effective soil water potential ($\psi_{\text{soil_effect MD}}$), sunlit leaf water potential ($\psi_{\text{sunlitleaf MD}}$), stomatal
347 conductance (G_{SMD}), and whole plant hydraulic conductance ($K_{\text{soil_plant MD}}$) at midday at several times during
348 the growing season are presented in Figures 8 and 9 for 2017 and 2018, respectively. As expected, there
349 was not much difference in terms of $\psi_{\text{soil_effecMD}}$ among F1P3, F2P2, and F2P3 from 02 August to one week
350 before harvest in 2017. The lowest $\psi_{\text{soil_effec MD}}$ was observed in the F1P2. Leaf water potential dropped
351 drastically but also $K_{\text{soil_plant MD}}$ increased strongly whereas $\psi_{\text{soil_effec MD}}$ remained quite similar (e.g. 18 July).
352 This is because sap flow have increased substantially in this day (e.g. from 2.34 mm d⁻¹ on 17 July to 6.97
353 mm d⁻¹ on 18 July for the F1P2). The stomatal conductance decreased a lot in this day which could be
354 explained that the atmospheric demand increased (e.g. global radiation was 13.6 MJ m⁻² on 17 July
355 compared to 23.9 MJ on 18 July while daily VPD was 0.7 kPa and 1.2 kPa, respectively) even more than the
356 sap flow. Midday sunlit leaf water potential was not distinctively different among treatments with the
357 lowest $\psi_{\text{sunlitleaf MD}}$ around -1.6 MPa throughout season. Also, G_{SMD} was rather similar among plots. The
358 $K_{\text{soil_plant MD}}$ ranged from 0.125 to 0.96 mm h⁻¹ MPa⁻¹ with a sharp reduction before harvest. In general, the
359 lowest values of $K_{\text{soil_plant MD}}$ were found in F1P2 which was consistent with the smaller overall seasonal
360 $K_{\text{soil_plant}}$ (as the slope of linear relationship between sap flow and difference of effective soil water potential
361 and sunlit leaf water potential) (see Supplementary material 5).

362 [Insert Figure 8 here]

363 The $\psi_{\text{soil_effec MD}}$ was substantially different in the two soil types and water treatments in 2018 (Figure 9a).
364 Both F1P2 and F1P3 showed a gradual drop of $\psi_{\text{soil_effec MD}}$ from 15 June until the third week of July then
365 increased after irrigation events on 18 July (Supplementary material 2b). However, $\psi_{\text{soil_effec MD}}$ of F1P2 was
366 much lower than F1P3 toward the harvest. The $\psi_{\text{soil_effec MD}}$ of F2P2 and F2P3 only decreased progressively
367 from around 10 July till harvest even though there was water supply from the irrigation (Supplementary

368 material 2b). The water applied by irrigation and coming in by rainfall were insufficient to wet up the
369 deeper soil layers which remained dry. The low G_{sMD} was corresponding to the lowest $\psi_{sunlitleaf MD}$ and
370 $K_{soil_plant MD}$ from the F1P2 (Figure 9c & 9d). The $K_{soil_plant MD}$ from all plots was ranging from 0.12 to 0.91 mm
371 $h^{-1} MPa^{-1}$. There was the drop in $K_{soil_plant MD}$ (i.e. 3 to 9 July or 17-18 July) before irrigation in this plot.
372 However, it increased after the irrigation (i.e. 10 July and 19 July). This suggests that K_{soil_plant} depends
373 strongly on the soil water content and the conductivity of the rhizosphere.

374 [Insert Figure 9 here]

375 **3.2.3. Relationships of stomatal conductance, transpiration, photosynthesis with plant hydraulic** 376 **variables at the plant canopy level**

377 The slope of linear relationship between sap flow and difference of ψ_{soil_effec} and $\psi_{sunlitleaf}$ is shown for three
378 consecutive days (leaf water potential measurements from the predawn) and before and after irrigation
379 applications (17, 18, and 19 July 2018 ~~or DOY 198, 199 and 200, respectively~~) (Figure 10). On both ~~DOYs~~
380 ~~dates 198-17 and 18 July and 199~~, the difference between ψ_{soil_effec} and $\psi_{sunlitleaf}$ was around -1.6 MPa with
381 very low transpiration rates in the treatment F1P2 which was associated with very low plant hydraulic
382 conductance and leaf curling. The whole plant hydraulic conductance was disrupted on these two days
383 (0.06 and 0.16 $mm h^{-1} MPa^{-1}$ for ~~17 and 18 July DOY 198 and 199~~, respectively). Water was supplied on ~~DOY~~
384 ~~18 July 199~~ at 1 PM for the irrigated plots (F1P3, F2P3) as well as F1P2 at 4 PM (for saving plant from death
385 due to severe drought stress). K_{soil_plant} was slightly changed (0.43 and 0.57 $mm h^{-1} MPa^{-1}$ for F1P3 on ~~DOY~~
386 ~~199-18 and 19 and 200 July~~, respectively and 0.5 and 0.58 $mm h^{-1} MPa^{-1}$ for F2P3 on ~~18 and 19 July DOY 199~~
387 ~~and 200~~, respectively). However, the increase of K_{soil_plant} was substantial in the F1P2 after the irrigation.
388 Soil water replenishment and an increase in the root - soil contact (Fig. 9a) allowed the K_{soil_plant} to recover
389 overnight to 0.46 $mm h^{-1} MPa^{-1}$. This resulted in a narrower water potential gradient between root zone
390 and sunlit leaf and in a higher transpiration rate on ~~19 July DOY 200~~.

391 [Insert Figure 10 here]

392 Seasonal average of different midday hydraulic conductance components (root system hydraulic
393 conductance - $K_{\text{soil_root}}$, stem hydraulic conductance - K_{stem} , and whole plant hydraulic conductance -
394 $K_{\text{soil_plant}}$) are shown in Figure 11. In the same year, the K_{stem} was not much different among F1P3, F2P2, and
395 F2P3 plots. The K_{stem} of those plots was slightly higher than in the F1P2 in both years. In general, the $K_{\text{soil_root}}$
396 was lower than the K_{stem} . Overall, the estimated $K_{\text{soil_plant}}$ was around $1/(1/K_{\text{soil_root}} + 1/K_{\text{stem}})$ regardless of
397 soil types, years, and water treatments. The $K_{\text{soil_root}}$ and $K_{\text{soil_plant}}$ in the F1P2 in 2018 was much lower than
398 the remaining plots while the $K_{\text{soil_root}}$ and $K_{\text{soil_plant}}$ ~~was-were~~ not much different among plots in 2017. Our
399 results indicated that there was an impact of soil hydraulic conductance on $K_{\text{soil_root}}$ and $K_{\text{soil_plant}}$. The
400 $K_{\text{soil_plant}}$ and $K_{\text{soil_root}}$ depend strongly on the soil water content and the soil hydraulic properties. Overall,
401 the estimated $K_{\text{soil_plant}}$ was around $1/(1/K_{\text{soil_root}} + 1/K_{\text{stem}})$ regardless of soil types, years, and water
402 treatments. Although there is a large difference in total root length between the two soil types (e.g. F1P3
403 versus F2P2 or F2P3 versus F2P2), $K_{\text{soil_root}}$ and $K_{\text{soil_plant}}$ in those two plots were not much different. This
404 could be explained by the fact that $K_{\text{soil_plant}}$ was not only depended on root length but also depended on
405 the variability of root segment hydraulic conductance. ~~The $K_{\text{soil_plant}}$ and $K_{\text{soil_root}}$ depend strongly on the soil~~
406 ~~water content and the soil hydraulic properties.~~ ~~Therefore, $K_{\text{soil_plant}}$ and $K_{\text{soil_root}}$ were not only a plant~~
407 ~~property but also a soil property.~~

408 [Insert Figure 11 here]

409 3.3. Relative importance of root and leaf area growth to transpiration and crop performance at canopy 410 level

411 Drought stress was observed in the rainfed plot (F2P2) in the second week of June 2017 with mild leaf
412 rolling. The crop then recovered due to sufficient rainfall and lower evaporative demand. Drought stress
413 occurring again at the stem elongation phase caused reduction of plant size (height and stem diameter)

414 (Supplementary material 4) as well as a slight reduction of leaf area and biomass in this plot
415 (Supplementary material 3a & 3c). Transpiration per unit of leaf area did not differ much among water
416 treatments and soil types in 2017 (Figure 12). The opposite was the case for the transpiration rate per unit
417 of root length. The observed root length at different soil depths (Figure 2) and total root length for two
418 plots in the stony soil was much smaller than in the silty soil (Figure 3). Therefore, transpiration per unit
419 of root length in the stony soils (F1P2 & F1P3) was almost 3 times higher than transpiration in the silty soil.
420 For the same soil, transpiration per unit root length of the irrigated treatment was slightly larger than in
421 the rainfed plot.

422 [Insert Figure 12 here]

423 The differences in sap flow per plant between water treatments and soil types were more pronounced in
424 2018 (Figure 13). The highest transpiration rate was observed in the irrigated plots (F1P3 & F2P3), followed
425 by the rainfed plot of the silty soil (F2P2) and it was lowest in the rainfed plot of the stony soil (F1P2).
426 These observations were in line with the differences in biomass and leaf area index between the
427 treatments (Supplementary material 3b & 3d) and plant size (Supplementary material 4b-c-d). In 2018,
428 severe leaf rolling was observed in the rainfed plot (F1P2) from the beginning of June until the end of the
429 growing period in 2018 (Supplementary material 3d). Similar to 2017, transpiration per unit of root length
430 was much higher in the stony plots as compared to silty plots. Also, for the silty soil, transpiration per unit
431 of root length of the irrigated plot (F2P3) was higher than in the rainfed plot (F2P2).

432 [Insert Figure 13 here]

433 Higher cumulative transpiration in the irrigated plots did not result in higher transpiration use efficiency
434 (TUE) in both soil types (Figure 14). For instance, TUE were 16.87 g mm^{-1} and 15.59 g mm^{-1} for F1P2 and
435 F2P2, respectively, while they were 15.47 and 14.79 g mm^{-1} for F1P3 and F2P3, respectively, in 2017 (Figure
436 14A). For the same soil, the rainfed plot showed slightly higher TUE than the irrigated plot. When
437 comparing the TUE of maize of the two soil types for the same water treatment, TUE at the stony soil was

438 almost the same in silty soil. The TUE was not much different among treatments and soil types in 2018.

439 Overall, TUE in 2017 was higher as compared to 2018 (Fig. 14b).

440 [Insert Figure 14 here]

441 4. Discussions

442 4.1. Effects of soil types, water application, and climatic condition on root growth

443 Our root observations showed that soil type considerably affected root growth more than water treatment
444 (Figure 2). Root growth was strongly inhibited by the stony soil where much lower root length was
445 observed than in the silty soil, especially in the deeper soil layers. This was consistent with the findings
446 reported in (Morandage et al., 2021) where a linear increase of stone content resulted in a linear decrease
447 of rooting depth across all stone contents and developmental stages. Also, both simulations and

448 observations indicated that rooting depth was ~~sensitive-increased due~~ to the presence of cracks in the
449 lower minirhizontron facility (Morandage et al., 2021) which could explain the high root length between

450 40 and 120 cm soil depths which was observed in the silty soil in both years. ~~In the silty soil, root growth
451 was favored towards deeper soil layers as also reported for the same field in 2016 for winter wheat
452 (Nguyen et al., 2020). Observation in field grown maize, the higher root length density and root diameter
453 were found in the sand than in the loam. This was attributed to the higher investment in nutrient
454 exploration because the lower concentration of plant available nutrients was in sand than in loam
455 (Vetterlein et al., 2022). Also, the larger root diameters in sand than in loam are more likely explained by
456 the need for soil contact of the roots (Jorda et al., 2022; Vetterlein et al., 2022).~~

457 ~~Our total root length was in the reported range of Cai et al., (2018) who studied winter wheat roots on the
458 same soil types in 2016. The total root length in our work was higher than the reported results from Cai
459 et al., (2018) especially in the rainfed plot of the silty soil (F2P2) in 2018 (Fig. 3). In terms of the ratios of
460 root length to shoot biomass:shoot ratio, our observations were in line with those reported in the~~

461 ~~same soil types for wheat in Cai et al., (2018).~~ Ordóñez et al., (2020) has reported much larger figures of
462 for instance 880 cm g⁻¹ in different locations and under different N application rates in maize growing in
463 the Midwest of US. Jorda et al., (2022) reported a wide range of ratios of root length to shoot biomass
464 ~~root: shoot ratio~~ from 200 to 1000 cm g⁻¹ around flowering time of maize depending on the wild type and
465 root hair mutant genotypes growing on either loamy or sandy soils. More roots and higher ratios of root
466 length to shoot biomass~~root: shoot ratios~~ were found in the sand than in the loam in both wild type and
467 root hair mutant genotypes (Jorda et al., 2022; Vetterlein et al., 2022). Cai et al., (2018) observed much
468 larger ratios of root length to shoot biomass ~~root: shoot ratio~~ in drought stressed plots than in irrigated
469 plot in both soil types in winter wheat which indicated the alternation of sink: source relationships to cope
470 with water stress. This study emphasized that more assimilates are used to promote root growth and
471 extract more water under drought stress. However, this was not the case for the stony soil in our work
472 where the drought stress was more pronounced, especially in 2018. ~~A slightly higher root: shoot ratio in~~
473 ~~the F1P2 treatment compared to F1P3 (DOY 194 & 255) was observed in 2017 while the root: shoot ratio~~
474 ~~in the two treatments was almost the same on DOY 199 and 228 in 2018 (Fig. 3). We only observed much~~
475 ~~higher root: shoot ratio in the rainfed plot (F2P2) as compared to the irrigated plot on the silty soil (F2P3).~~
476 ~~Comas et al., (2013) has reported that maize increases the ratio of root to leaf surface area and relative~~
477 ~~distribution to deeper depths in responses to water deficit. Under drought stress, root growth of maize~~
478 ~~continues longer into the season than shoot and vegetative growth and even beyond the onset of~~
479 ~~reproduction.~~ A drop of soil water potential (Supplementary material 2b), thus effective soil water
480 potential (Figure 8a) was substantial from 10th July 2018 toward the harvest in the rainfed plot in the silty
481 soil (F2P2) which was consistent with the reduction of leaf water potential (Fig. 8b), leaf area
482 (Supplementary material 3c), total dry matter (Supplementary material 3d), and crop height
483 (Supplementary material 4b) as compared the irrigated plot (F2P3). This indicates a mild water stress in
484 2018 in the rainfed plots on the silty soil. The larger ratios of root length to shoot biomass ~~root: shoot ratio~~
485 in this F2P2 plot in 2018 as compared to F2P3 could be explained by the change of source: sink relations

486 where more assimilates were devoted to root growth, even at a later growth stage. Moreover, the low
487 stone content and soil cracks (Morandage et al., 2021) might favor root growth in the deeper soil layers
488 which are close to the ~~lower-shallow~~ soil water table in the ~~rhizotrone facility site~~ with silty soil
489 (Vanderborght et al., 2010). In conclusion, both soil texture and water conditions influenced the root
490 growth, however, effects of the former on root length was more pronounced than the latter.”

491 **4.2. Effects of soil types, water application, and climatic condition on stomatal conductance,** 492 **photosynthesis, transpiration, leaf water potential, and plant hydraulic conductance**

493 **4.2.1. Leaf water potential and stomatal conductance as affected by soil water conditions**

494 ~~In our study, stomata closed earlier and at more negative soil and leaf water potentials in stony soil than~~
495 ~~in silty soil (see Fig. 4, 5, 6 and 7).~~ In ~~other-the previous~~ work, Koehler et al., (2022) reported that maize
496 stomata closed at lower negative leaf water potentials in sand than in loam growing under controlled
497 environment. Cai et al., (2022b) investigated transpiration response of pot-grown maize in two contrasting
498 soil textures (sand and loam) and exposed to two consecutive VPD levels (1.8 and 2.8 kPa). Transpiration
499 rate decreased at less negative soil matric potential in sand than in loam at both VPD levels. In sand, high
500 VPD generated a steeper drop in stomatal conductance with decreasing leaf water potential which
501 indicated that the transpiration and stomatal responses depend on soil hydraulics. In our study, stomata
502 closed earlier and at more negative soil and leaf water potentials in the stony soil than in the silty soil (see
503 Fig. 4, 5, 6 and 7). The lower soil water holding capacity of the stony soil compared to the silty soil resulted
504 in lower soil water potential and smaller total plant hydraulic conductance which in turn led to earlier
505 stomatal closure and to more negative soil water potential in the stony soil.

506 Stomatal control is an early and effective response to water stress to prevent the plant from water loss
507 and dehydration. Maize is considered as an isohydric plant which closes its stomata to maintain leaf water
508 potential above critical levels (Tardieu and Simonneau, 1998). Our results showed that minimum leaf

509 water potential varied among treatments (-1.5 MPa for F1P3, F2P2, and F2P3 and up to -2 MPa for F1P2
510 in 2017, while in 2018 minimum values were -2 MPa for F2P3, F2P2, and F2P3 and -2.7 MPa for F1P2) (Fig.
511 7 and Fig. 8, Fig. 9). Large variability of minimum LWP has been reported for maize genotypes. Leaf water
512 potential can be limited at quite high values, for instance -0.8 MPa in some lines of maize, while values as
513 low as -1.5 MPa have also been recorded (Welcker et al., 2011). Some drought-tolerant maize genotypes
514 close stomata at less negative leaf water potential under soil water depletion than more sensitive ones,
515 which is associated with their ability to avoid xylem embolism and hydraulic failure (Cochard, 2002; Tyree
516 et al., 1986; Li et al., 2009). However, our results show that the leaf water potential threshold can vary
517 within the same genotype depending on soil types, climatic conditions and water management. It should
518 be noted the constant ψ_{leaf} level (around -1.8 MPa) under different soil water regimes reported in Tardieu
519 and Simonneau (1998) that was associated with high VPD values, was based on observations from a single
520 day. Measurements on ψ_{leaf} and Gs for different days during several growing seasons have been rarely
521 reported for maize. The results of our study confirmed that maize appears to maintain its ψ_{leaf} at around -
522 1.5 to -2 MPa which depended on evaporative demand and levels of soil moisture (Fig. 1, Fig. 7, Fig. 8, and
523 Fig. 9). This has been reported recently in Nguyen et al. (2022a). Our current study, which investigates the
524 drivers of the modifications of ψ_{leaf} during the growing season, also confirmed that such stomatal
525 regulation and the ψ_{leaf} were mediated by soil hydraulics. Cochard, (2002) reported that stomatal closure
526 is complete between -1.6 and -2 MPa. In our study, the observed ψ_{leaf} was below -2 MPa for several days.
527 Similar values were also reported by Li et al. (2002) for field-grown maize in semiarid conditions. In our
528 study, leaf water potential dropped below -2 MPa in the rainfed plots to levels much lower than those
529 observed in the irrigated plots in 2018. This could imply different degrees of isohydry in maize. A
530 continuum exists in the degree to which stomata regulate the ψ_{leaf} for trees (Domec and Johnson, 2012;
531 Klein, 2014) or in grape-vine (Schultz, 2003). Also, cultivars of grape vine show large differences in
532 minimum ψ_{leaf} indicating differing degrees of isohydric behavior (Coupel-Ledru et al., 2014). When
533 comparing different herbaceous species, Turner et al., (1984) showed that there was a range of isohydric

534 behavior among the species in terms of the response to increasing vapor pressure deficit (VPD) under
535 sufficient soil moisture. However, conclusions concerning contrasting minimum ψ_{leaf} between 2017 and
536 2018 should not be overemphasized. Observed extremely low ψ_{leaf} correspond with the extremely low Gs
537 and were further accompanied by complete leaf curling in rainfed treatment under stony soil in 2018 (Fig.
538 4, 5, and Fig. 9) due to the extremely dry and hot summer and severe soil dryness. In conclusion, our results
539 confirmed that the minimum ψ_{leaf} not only depended on genotypic differences but also was influenced by
540 soil types and soil hydraulic conductance.

541 4.2.2. Hydraulic conductance components as affected by soil water conditions

542 Estimates of hydraulic components in soil-plant-atmosphere continuum are important not only to
543 understand its underlying relationship to other crop characteristics (stomatal conductance,
544 transpiration, and photosynthesis) but also to provide modeling parameters in process-based soil-root-
545 shoot models (Nguyen et al., 2020; Sulis et al., 2019; Nguyen et al., 2022b). Measurement of the
546 components of hydraulic conductance are challenging under field conditions because it requires the
547 estimation of transpiration and root to leaf water potential gradients. To our knowledge, our results were
548 unique with regard to the dynamics of $K_{\text{soil_plant}}$ for field-grown maize on two soil types and under
549 contrasting water, and climate conditions. Our seasonal $K_{\text{soil_plant}}$ ranged from 0.12 mm h⁻¹ MPa⁻¹ to 0.9 mm
550 h⁻¹ MPa⁻¹ (Fig. 8 & Fig. 9; Fig. 10, and Supplementary material 5). Root system hydraulic conductance
551 ranged from 0.26 to 1.47 mm h⁻¹ MPa⁻¹ (Figure 11). Note that the unit of $K_{\text{soil_plant}}$ as mm h⁻¹ MPa⁻¹ could
552 be equivalent to the unit of 10⁻⁵ h⁻¹ if one assumes 1MPa is approximately 10⁵ mm in terms of pressure
553 head. Cai et al., (2018) reported root hydraulic conductance in winter wheat from 0.05 ~~×10⁻⁵h⁻¹~~ to 0.5 mm
554 h⁻¹ MPa⁻¹ ×10⁻⁵h⁻¹ in two similar soil types. Nguyen et al., (2020) also reported $K_{\text{soil_plant}}$ in winter wheat
555 from 0.0625 ~~×10⁻⁵h⁻¹~~ to 0.461 mm h⁻¹ MPa⁻¹ ×10⁻⁵h⁻¹. Meunier et al., (2018) focused on estimating the
556 root system hydraulic conductance of maize in a container experiment where the range of $K_{\text{soil_plant}}$ was
557 much larger from 0.37 ~~×10⁻⁵h⁻¹~~ to 36 mm h⁻¹ MPa⁻¹ ×10⁻⁵h⁻¹ for the plant density of 10 plant m⁻². Jorda et

558 al., (2022) estimated root system hydraulic conductance of 0.5 to $1.5 \cdot 10^{-3} \text{ d}^{-1}$ which would be roughly
559 between 2 to $6 \text{ mm h}^{-1} \text{ MPa}^{-1} \cdot 10^{-5} \text{ h}^{-1}$. ~~To simulate leaf water potential in the modeling work for field maize,~~
560 ~~Nguyen et al., (2022b) based on assumption that $K_{\text{soil_plant}}$ was $0.53 \times K_{\text{soil_root}}$. Such fraction (0.53) was~~
561 ~~consistent with the reported range in our work (0.3–0.8) with average $K_{\text{soil_plant}}$ was at half of root system~~
562 ~~hydraulic conductance across treatments.~~ In our work, except the F2P2 in 2018, the stem hydraulic
563 conductance was 10% to 60% higher than root system hydraulic conductance. Gallardo et al., (1996)
564 reported that stem hydraulic conductance of wheat was lower than root system conductance at around
565 71 to 91 days after sowing (DAS), but they were similar at 102 DAS. In lupine, stem hydraulic conductance
566 was two times higher than root system conductance regardless of measured days. The larger root length
567 in wheat than lupine did not necessarily result in higher root conductance in wheat. Together with this
568 study, our study emphasizes the values of stem hydraulic conductance compared to the root hydraulic
569 conductance in maintaining water potential gradient from shaded leaf or plant color to the sunlit leaf.

570 Our results showed clear differences in $K_{\text{soil_plant}}$ among treatments where much lower $K_{\text{soil_plant}}$ was
571 observed in the F1P2 as compared to F2P2 (see Figure 10 for 2018; Figure 8 and 9 and Supplementary
572 material 5 for both years). This indicated the soil texture dependence for whole plant hydraulic
573 conductance. Maize plants with the shorter root system (i.e. rainfed plot in the stony soil in 2018) (Fig. 3)
574 had lower plant hydraulic conductance. Our results indicated that there was an impact of soil hydraulic
575 conditions on $K_{\text{soil_plant}}$ via the reduction of root system hydraulic conductance. Our analysis for three
576 consecutive measurement days in 2018 (Fig 10) showed that in the silty soil, $K_{\text{soil_plant}}$ decrease when soil
577 water potentials are becoming more negative. For instance, in the silty soil in 2018 when the soil water
578 potentials were considerably lower in the rainfed than in the irrigated plot (e.g. after 10th July), $K_{\text{soil_plant}}$
579 was lower in the rainfed than in the irrigated plot. In the stony soil, the $K_{\text{soil_plant}}$ and leaf water potentials
580 seems to decrease more considerably (compared to the silty soil) when the soil water potentials become
581 more negative. In other words, $K_{\text{soil_plant}}$ increased considerably when the soil water potentials in the stony

582 soil increased. Koehler et al., (2022) analyzed the maize plant responses to soil drying under controlled
583 climate conditions with three soil types (sand, sandy loam, and loam). This study confirmed the impact of
584 soil texture on plant response to soil drying in various relationships. In their work, the soil-plant
585 conductance decreased in both sand and loam but at less negative water potentials in the sand than in the
586 loam. Root system hydraulic conductance decreased at less negative bulk soil water potential in the coarse
587 soil than in the fine soil (Vanderborght et al., 2023). In our work, $K_{\text{soil_plant}}$ increased slowly after irrigation
588 mainly for the severe water stress plot (see F1P2 on 19 July in Fig 9d and 10c). This implied that added soil
589 water by irrigation took some time for recovery the soil-root contact within the rhizosphere.

590 **4.2.3. Relationships of stomatal conductance, transpiration, photosynthesis with plant hydraulic** 591 **variables**

592 In 2017, our estimated midday effective soil water potential ($\psi_{\text{soil_effec MD}}$) did not vary much (between soil
593 types and treatments) which was consistent with the low variability in midday sunlit leaf water potential
594 ($\psi_{\text{sunlitleaf MD}}$) and $K_{\text{soil_plant}}$ among water treatments (Fig. 8). The $\psi_{\text{soil_effec MD}}$ was high (around -0.35 MPa)
595 while $\psi_{\text{sunlitleaf MD}}$ was around -1.5 MPa (Fig. 8c). In contrast, the difference of $\psi_{\text{soil_effec MD}}$, $\psi_{\text{sunlitleaf MD}}$, and
596 $K_{\text{soil_plant}}$ was higher among water treatments and soil types in 2018 as compared to 2017. Moreover, the
597 high VPD and air temperature in combination with the small precipitation in the main growing season in
598 2018 led to a stronger reduction of $\psi_{\text{soil_effec MD}}$ up to -0.75 MPa (i.e. in F1P2 in the stony soil on 17 and 18
599 July in 2018, Figure 9) and $\psi_{\text{sunlitleaf MD}}$ to -2.5 MPa. This low $\psi_{\text{soil_effec MD}}$ in F1P2 was associated with low
600 stomatal conductance (Fig. 9c), low $K_{\text{soil_plant}}$ (Fig. 9d), and strong transpiration reduction (Fig. 10a-b, Fig.
601 12, and Supplementary material 5). Our results were in line with the analysis from Cai et al., (2022a) which
602 revealed that water uptake depended on effective soil water potential which in turn depended on soil
603 water potential which differed between plots with different textures.

604 The transpiration rate and $K_{\text{soil_plant}}$ (slope of linear regression lines in Fig. 10a and b) were very low in the
605 rainfed plot under the stony soil (F1P2) which was associated with the large $\psi_{\text{difference}}$ (Fig. 10a & b) and the

606 lower stomatal conductance as compared to other plots (Fig. 9c). The $K_{\text{soil_plant}}$ slightly increased after
607 irrigation (18 July - DOY 199 in Fig. 10b) corresponding with the smaller $\psi_{\text{difference}}$ (Fig. 10b) and an increase
608 in stomatal conductance (Fig. 9c). Seasonal $K_{\text{soil_plant}}$ was low in the rainfed plot under stony soil (F1P2) with
609 the larger $\psi_{\text{difference}}$ (Supplementary material 5). In addition, our study showed that the midday stomatal
610 conductance, photosynthesis, and transpiration were significantly correlated only with midday $K_{\text{soil_plant}}$ in
611 the rainfed plot on the stony soil (F1P2) in 2018 where high VPD and temperature occurred
612 (Supplementary material 6, 7, and Supplementary material 8). Maize plants had lower plant hydraulic
613 conductance and more negative soil water potential in the rainfed plot in stony soil ~~required the larger~~
614 ~~gradients in soil water pressure to sustain the same transpiration rate (that thus and they~~ exhibited earlier
615 stomatal closure) as compared to the same plot in the silty soil. This was in line with a study from Abdalla
616 et al., (2022) which suggested that during soil drying, stomatal regulation of tomato is controlled by root
617 and soil hydraulic conductance. Recent work from Müllers et al., (2022) on faba bean and maize suggested
618 that differences in the stomatal sensitivity among plant species can be partly explained by the sensitivity
619 of soil-plant hydraulic conductance to soil drying. The loss of conductance has immediate consequences
620 for leaf water potential and the associated stomatal regulation. Cai et al., (2022b) also showed that the
621 decrease in sunlit leaf stomatal conductance was well correlated with the drop in soil-plant hydraulic
622 conductance, which was significantly affected by soil texture. This was confirmed in our work where the
623 stony soil strongly impacted on root growth, modulated $K_{\text{soil_plant}}$, and consequently influenced the leaf
624 stomatal conductance, photosynthesis, and transpiration.

625 **4.3. Relative contribution of water control by leaves and roots on transpiration and transpiration use** 626 **efficiency**

627 Responses of crops via stomatal control to reduce water loss at leaf scale while maintaining leaf
628 photosynthesis and water use efficiency were reported earlier (Nguyen et al., 2022a; Vitale et al., 2007).
629 In addition to that, in the maize experiments in 2017 and 2018 leaf rolling was observed in both rainfed

630 plots on the stony and the silty soil in the second week of June 2017 and from the beginning of June until
631 the end of the growing period in 2018. This indicates another dehydration avoidance mechanism resulting
632 from morphological adjustments which is an effective mechanism for delaying senescence (Aparicio-Tejo
633 and Boyer, 1983; Richards et al., 2002). Stomatal closure resulted in more reduction of transpiration and
634 assimilation in the rainfed plots than irrigated plots with the same soil type (Fig. 5, Fig. 6, Fig. 7, and Fig.
635 13A). There was reduction of shoot biomass (also stem size and leaf size adjustments) in F1P2 as compared
636 to other plots. However, the TUE was not smaller in this plot than the remaining plots. These observations
637 confirm that plant size adjustments through reduction of height, leaf width and length are efficient
638 responses to reduce water loss at canopy scale in addition to stomatal control at the leaf level.

639 Relative contribution of leaf area to transpiration has been highlighted in wheat where reduction of tiller
640 number resulted in significantly (lower LAI, thus lower canopy transpiration (Cai et al., 2018; Trillo and
641 Fernández, 2005; Nguyen et al., 2022a). However, root system conductance per unit of leaf area and per
642 unit root mass were strongly reduced and eventually more than reduction of leaf area under water stress
643 (Trillo and Fernández, 2005). In our work, expressing the transpiration per unit of root length on the one
644 hand allowed to analyze the role of total root length to water uptake. However, on the other hand, the
645 lower total root length did not necessarily result in a lower root water uptake and vice versa. For instance,
646 the rainfed plot of the treatment F2P2 had the larger total root length which could postpone the effect of
647 soil water limitations in drying soils due to greater ability to extract water from subsoils. Therefore,
648 transpiration was very similar between F2P2 and F2P3. Despite of the much lower total root length in the
649 stony soil, K_{soil_plant} in the irrigated plot (F1P3) was not much lower than in the same water treatment in
650 the silty soil (F2P3, Fig. 8c, 9c, Fig. 10, and Supplementary material 5). This could be explained by the fact
651 that the K_{soil_plant} variability was not only depended on root architecture (here the root length and
652 distribution) but also depended on the variability of root segment hydraulic properties which has also been
653 illustrated and discussed in Zwieniecki et al. (2002), Frensch and Steudle (1989), Meunier et al. (2018),

654 Couvreur et al. (2014), and Ahmed et al. (2018). Meunier et al. (2020) showed that more than 65% of the
655 variability of root system conductance of maize plants could be attributed to variability in root
656 architecture, which includes root length, whereas only 25% of the variability was attributed to root
657 segment hydraulic properties. However, the analysis of Meunier et al., (2020) neither included the impact
658 of root hairs nor the impact of rhizosphere conductivity but only focused on the root system hydraulic
659 conductance. Moreover, the contribution of shoot hydraulic conductance could be large in plants (Gallardo
660 et al., 1996; Trillo and Fernández, 2005; Sunita et al., 2014) which also confirmed in our work. In our work,
661 K_{soil_plant} comprised root and shoot conductance which are directly influenced by soil hydraulics. Our
662 estimates of K_{soil_plant} varied with transpiration and gradients of $\psi_{sun\text{littleaf}}$ and ψ_{soil_effec} . Thus, any change of
663 soil hydraulic conductance will change the root to shoot water potential. Consequently, it will affect the
664 gradients between shoot and root rhizosphere (Carminati and Javaux, 2020). Thus, our study is revealing
665 the importance of both soil texture characteristics and root phenotypic traits (here root length) in
666 regulating plant transpiration (Cai et al., 2022a). Other traits like root hair density (Cai et al., 2022a) or
667 higher root length density (Vadez, 2014) could contribute to the soil to root water potential and root-zone
668 hydraulic conductance where dense root hairs are delaying soil water deficit in drying soils. However,
669 contrasting results have shown that root hairs did not have an effects on root water uptake (see Jorda et
670 al. 2022). The role of root hairs could not be analyzed in our work which was based on the root data from
671 minirhizotron images.

672 5. Conclusion

673 We presented plant hydraulic characteristics and crop growth from root to shoot of maize under field-
674 grown conditions with two soil types (silty and stony), each soil with two water regimes (irrigated and
675 rainfed) for two growing seasons (2017, 2018). Our results confirmed that root length and ratios of root
676 length to shoot biomass~~root:shoot ratio was were~~ modulated by soil types and water treatment but less
677 by seasonal evaporative demand. Increase ratio of root length to shoot biomass~~root:shoot ratio~~ has been

678 an important response of maize that allows plants to extract more water under drought stress that
679 occurred rather in the silty soil but less in the stony soil due to the higher content of stony material. Despite
680 of lower root length in the stony irrigated plot, transpiration rate was not much lower than in the silty
681 irrigated plot. This could be related to another property of the root such as root segment conductance or
682 other root traits (e.g. root hair). Further investigation with extensive measurements of roots including axial
683 and radial root conductance at field scale will be required to better explain the observed results.

684 Another conclusion is that stomatal regulation maintains leaf water potential at certain thresholds which
685 depends on soil types, soil water availability, and seasonal atmospheric demand. The stomata conductance
686 was smaller and decreased at more negative leaf water potentials in stony soil than in silty soil. The leaf
687 water potentials are affected by the soil-plant ~~plant~~ hydraulic conductance. In addition to stomatal
688 regulation, leaf growth and plant size adjustments are important to regulate the transpiration ~~that and~~
689 water use efficiency ~~was not different among treatments and soil types~~ in the same year.

690 The lowest soil-plant hydraulic conductance was observed in the stony soil with severe drought stress as
691 compared to silty soil while its variation depends also on the soil water variation (before and after
692 irrigation). Root system and soil-plant hydraulic conductance depended strongly on soil hydraulic
693 properties. In the stony soil, which has a considerably smaller water holding capacity than the silty soil,
694 root length was considerably smaller than in the silty soil. Nevertheless water uptake per unit root length
695 was much larger than in the fine soil. This also means that the hydraulic conductance per unit root length
696 must have been much larger in the stony soil than in the fine soil. Cai et al., (2018) observed a similar effect
697 for winter wheat but they found much smaller differences in the root length normalized root conductance.
698 The higher root length normalized root conductance means that the anatomy of the root tissues must
699 have been influenced by the soil texture and compensated the considerably smaller root length in the
700 stony soil. Looking at the effect of water treatments in the silt soil, the non-irrigated plot had more roots
701 than the irrigated one and both had more roots in the year with high VPD. But the soil-root conductance

702 was higher in the irrigated plot than in the rainfed plot. This means that in the irrigated plot, the soil-root
703 conductance per unit root length was higher than in the rainfed plot. This could either be due to wetter
704 soil conditions and higher soil conductance or it could be due to a larger conductance of the root tissues.
705 Especially in 2017 when the silty soil was wetter, the slightly larger soil-root conductance in the irrigated
706 plot is most likely the result of larger root tissue conductance in the irrigated plot. Thus, how root
707 architecture (here represented simply by the total root length) and root tissue conductivities 'respond' to
708 drought stress might be opposite depending on the comparisons that are made. When the stony soil and
709 silt soil are compared, the higher 'stress' due to lower water availability in the stony soil resulted in less
710 roots with a higher root tissue conductance in the soil with more stress. When comparing the rainfed with
711 the irrigated plot in the silty soil, the higher stress in the rainfed soil resulted in more roots with a lower
712 root tissue conductance in the treatment with more stress. This illustrates that the 'response' to stress can
713 be completely opposite depending on conditions or treatments that lead to the differences in stress that
714 are compared. Therefore, it cannot be the 'stress' alone that defines how a plant will react and adapt its
715 root system. Modelling the impact of stress and the feedback between drought stress and plant
716 development is likely controlled by other properties or parameters that change with changing soil water
717 availability and atmospheric water demand than the plant stress level. Results from this study show that
718 soil-crop models should focus not only on simulating stomatal regulations to capture the response to
719 drought stress, but also require adequate representations of leaf growth and adjustments.

720

721

722

723

724

725 **Acknowledgements**

726 This work has partially been funded by Federal Ministry of Education and Research (BMBF) through
727 European SUSCAP project – 031B0170B and COINS project} and the Deutsche Forschungsgemeinschaft
728 (DFG, German Research Foundation) under Germany’s Excellence Strategy – EXC 2070 – 390732324”. We
729 acknowledge the support by the SFB/TR32 “Pattern in Soil–Vegetation–Atmosphere Systems: Monitoring,
730 Modelling, and Data Assimilation” funded by the Deutsche Forschungsgemeinschaft (DFG). Thuy Nguyen
731 and Thomas Gaiser also thank the DETECT – CRC 1502 research program which is funded by DFG. We thank
732 Dr. Matthias Langensiepen for his supports and technical help in the TR32 project. We would like to thank
733 all the student assistants and technicians for their considerable efforts to collect the data in the field and
734 the laboratories.

735

736

737

738

739

740

741

742

743

744

745

746 **List of Tables**

747 Table 1. Crop phenology and management information for different treatments in 2017 and 2018.

Soil types	2017				2018			
	Stony (F1)	Stony (F1)	Silty (F2)	Silty (F2)	Stony (F1)	Stony (F1)	Silty (F2)	Silty (F2)
Water treatments	Rainfed (P2)	Irrigated (P3)	Rainfed (P2)	Irrigated (P3)	Rainfed (P2)	Irrigated (P3)	Rainfed (P2)	Irrigated (P3)
Plot names	F1P2	F1P3	F2P2	F2P3	F1P2	F1P3	F2P2	F2P3
Growing season (days) [‡]	136	136	136	136	107	107	107	107
Cumulative rainfall (mm) [*]	248.7	248.7	248.7	248.7	91.3	91.3	91.3	91.3
Irrigation (mm)	0	130	0	130	66	257.6	0	257.6
Fertilizer application (mm/dd) (per hectare)	05/09: 100 kg N + 40 kg P ₂ O ₅ 07/06: 80 kg N + 40 kg K ₂ O				05/22: 100 kg N 05/30: 40 kg P ₂ O ₅ + 40 kg K ₂ O 06/27: 80 kg N			
Sowing date (mm/dd)	05/04				05/08			
Emergence date	05/09				05/13			
Tasseling date	07/09				07/09			
Silking date	07/14				07/11			
Harvest date	09/12				08/22			

748 Notes: [‡] from sowing to harvest; ^{*} for rainfall for whole growing season;

749

750

751

752

753

754

755

756

757

758 **Reference**

- 759 Abdalla, M., M.A. Ahmed, G. Cai, F. Wankmüller, N. Schwartz, et al. 2022. Stomatal closure during water
760 deficit is controlled by below-ground hydraulics. *Ann. Bot.* 129(2): 161–170. doi:
761 10.1093/aob/mcab141.
- 762 Abdalla, M., A. Carminati, G. Cai, M. Javaux, and M.A. Ahmed. 2021. Stomatal closure of tomato under
763 drought is driven by an increase in soil-root hydraulic resistance. *Plant. Cell Environ.* 44(2): 425–
764 431. doi: 10.1111/pce.13939.
- 765 Ahmed, M.A., M. Zarebanadkooki, F. Meunier, M. Javaux, A. Kaestner, et al. 2018. Root type matters:
766 Measurement of water uptake by seminal, crown, and lateral roots in maize. *J. Exp. Bot.* 69(5): 1199–
767 1206. doi: 10.1093/jxb/erx439.
- 768 Aparicio-Tejo, P., and J.S. Boyer. 1983. Significance of Accelerated Leaf Senescence at Low Water Potentials
769 for Water Loss and Grain Yield in Maize1. *Crop Sci.* 23(6): crops1983.0011183X002300060040x. doi:
770 <https://doi.org/10.2135/cropsci1983.0011183X002300060040x>.
- 771 Bauer, F.M., L. Lärm, S. Morandage, G. Lobet, J. Vanderborght, et al. 2021. Combining deep learning and
772 automated feature extraction to analyze minirhizotron images: development and validation of a new
773 pipeline. *bioRxiv* (1): 2021.12.01.470811.
774 <https://www.biorxiv.org/content/10.1101/2021.12.01.470811v1%0Ahttps://www.biorxiv.org/content/10.1101/2021.12.01.470811v1.abstract>.
- 776 Bornemann*, L., M. Herbst, G. Welp, H. Vereecken, and W. Amelung. 2011. Rock Fragments Control Size
777 and Saturation of Organic Carbon Pools in Agricultural Topsoil. *Soil Sci. Soc. Am. J.* 75(5): 1898. doi:
778 10.2136/sssaj2010.0454.
- 779 Bourbia, I., C. Pritzkow, and T.J. Brodribb. 2021. Herb and conifer roots show similar high sensitivity to
780 water deficit. *Plant Physiol.* 186(4): 1908–1918. doi: 10.1093/plphys/kiab207.
- 781 Cai, G., M.A. Ahmed, M. Abdalla, and A. Carminati. 2022a. Root hydraulic phenotypes impacting water
782 uptake in drying soils. *Plant Cell Environ.* 45(3): 650–663. doi: 10.1111/pce.14259.
- 783 Cai, G., M. König, A. Carminati, M. Abdalla, M. Javaux, et al. 2022b. Transpiration response to soil drying
784 and vapor pressure deficit is soil texture specific. *Plant Soil* (0123456789). doi: 10.1007/s11104-022-
785 05818-2.
- 786 Cai, G., J. Vanderborght, V. Couvreur, C.M. Mboh, and H. Vereecken. 2017a. Parameterization of Root
787 Water Uptake Models Considering Dynamic Root Distributions and Water Uptake Compensation.
788 *Vadose Zo. J.* 0(0): 0. doi: 10.2136/vzj2016.12.0125.
- 789 Cai, G., J. Vanderborght, A. Klotzsche, J. van der Kruk, J. Neumann, et al. 2016. Construction of
790 Minirhizotron Facilities for Investigating Root Zone Processes. *Vadose Zo. J.* 15(9): 0. doi:
791 10.2136/vzj2016.05.0043.
- 792 Cai, G., J. Vanderborght, M. Langensiepen, A. Schnepf, H. Hüging, et al. 2018. Root growth, water uptake,
793 and sap flow of winter wheat in response to different soil water conditions. *Hydrol. Earth Syst. Sci.*
794 22(4): 2449–2470. doi: 10.5194/hess-22-2449-2018.
- 795 Cai, Q., Y. Zhang, Z. Sun, J. Zheng, W. Bai, et al. 2017b. Morphological plasticity of root growth under mild
796 water stress increases water use efficiency without reducing yield in maize. *Biogeosciences* 14(16):
797 3851–3858. doi: 10.5194/bg-14-3851-2017.

798 Carminati, A., and M. Javaux. 2020. Soil Rather Than Xylem Vulnerability Controls Stomatal Response to
799 Drought. *Trends Plant Sci.* 25(9): 868–880. doi: 10.1016/j.tplants.2020.04.003.

800 Carminati, A., M. Zarebanadkouki, E. Kroener, M.A. Ahmed, and M. Holz. 2016. Biophysical rhizosphere
801 processes affecting root water uptake. *Ann. Bot.* 118(4): 561–571. doi: 10.1093/aob/mcw113.

802 Choudhary, S., and T.R. Sinclair. 2014. Hydraulic conductance differences among sorghum genotypes to
803 explain variation in restricted transpiration rates. *Funct. Plant Biol.* 41(3): 270–275. doi:
804 10.1071/FP13246.

805 Cochard, H. 2002. Xylem embolism and drought-induced stomatal closure in maize. *Planta* 215(3): 466–
806 471. doi: 10.1007/s00425-002-0766-9.

807 Comas, L.H., S.R. Becker, V.M. V. Cruz, P.F. Byrne, and D.A. Dierig. 2013. Root traits contributing to plant
808 productivity under drought. *Front. Plant Sci.* 4(NOV): 1–16. doi: 10.3389/fpls.2013.00442.

809 Coupel-Ledru, A., É. Lebon, A. Christophe, A. Doligez, L. Cabrera-Bosquet, et al. 2014. Genetic variation in
810 a grapevine progeny (*Vitis vinifera* L. cvs GrenachexSyrah) reveals inconsistencies between
811 maintenance of daytime leaf water potential and response of transpiration rate under drought. *J.*
812 *Exp. Bot.* 65(21): 6205–6218. doi: 10.1093/jxb/eru228.

813 Couvreur, V., J. Vanderborght, X. Draye, and M. Javaux. 2014. Dynamic aspects of soil water availability for
814 isohydric plants: Focus on root hydraulic resistances. *water Resour. Res.* 50: 8891–8906. doi:
815 10.1002/2014WR015608.Received.

816 Couvreur, V., J. Vanderborght, and M. Javaux. 2012. A simple three-dimensional macroscopic root water
817 uptake model based on the hydraulic architecture approach. *Hydrol. Earth Syst. Sci.* 16: 2957–2971.
818 doi: 10.5194/hess-16-2957-2012.

819 Daryanto, S., L. Wang, and P. Jacinthe. 2016. Global Synthesis of Drought Effects on Maize and Wheat
820 Production. *PLoS One* 11(5): 1–15. doi: 10.1371/journal.pone.0156362.

821 Draye, X., Y. Kim, G. Lobet, and M. Javaux. 2010. Model-assisted integration of physiological and
822 environmental constraints affecting the dynamic and spatial patterns of root water uptake from
823 soils. *J. Exp. Bot.* 61(8): 2145–2155. doi: 10.1093/jxb/erq077.

824 Domec, J., and D.M. Johnson. 2012. Does homeostasis or disturbance of homeostasis in minimum leaf
825 water potential explain the isohydric versus anisohydric behavior of *Vitis vinifera* L. cultivars? *Tree*
826 32: 245–248. doi: 10.1093/treephys/tps013.

827 Domec, J., and M.L. Pruyn. 2008. Bole girdling affects metabolic properties and root, trunk and branch
828 hydraulics of young ponderosa pine trees. *Tree Physiol.* (28): 1493–1504.

829 Dynamax. 2007. *Dynagage Sap Flow Sensor User Manual.* 1–107. Last access on March 5th 2015.

830 Effendi, R., S.B. Priyanto, M. Aqil, and M. Azrai. 2019. Drought adaptation level of maize genotypes based
831 on leaf rolling, temperature, relative moisture content, and grain yield parameters. *IOP Conf. Ser.*
832 *Earth Environ. Sci.* 270(1). doi: 10.1088/1755-1315/270/1/012016.

833 Fang, J., and Y. Su. 2019. Effects of Soils and Irrigation Volume on Maize Yield, Irrigation Water Productivity,
834 and Nitrogen Uptake. *Sci. Rep.* 9(1): 1–11. doi: 10.1038/s41598-019-41447-z.

835 Frensch, J., and E. Steudle. 1989. Axial and Radial Hydraulic Resistance to Roots of Maize (*Zea mays* L.).
836 *Plant Physiol.* 91: 719–726.

837 Gallardo, M., J. Eastham, P.J. Gregory, and N.C. Turner. 1996. A comparison of plant hydraulic
838 conductances in wheat and lupins. *J. Exp. Bot.* 47(295): 233–239. doi: 10.1093/jxb/47.2.233.

839 Hochberg, U., F.E. Rockwell, N.M. Holbrook, and H. Cochard. 2018. Iso/Anisohydry: A Plant–Environment
840 Interaction Rather Than a Simple Hydraulic Trait. *Trends Plant Sci.* 23(2): 112–120. doi:
841 10.1016/j.tplants.2017.11.002.

842 Hopmans, J.W., and K.L. Bristow. 2002. Current Capabilities and Future Needs of Root Water and
843 Nutrient Uptake Modeling. In: Sparks, D.L.B.T.-A. in A., editor, *Advances in Agronomy*. Academic
844 Press. p. 103–183

845 Hubbard, R.M., M.G. Ryan, V. Stiller, and J.S. Sperry. 2001. Stomatal conductance and photosynthesis vary
846 linearly with plant hydraulic conductance in ponderosa pine. *Plant, Cell Environ.* 24(1): 113–121. doi:
847 10.1046/j.1365-3040.2001.00660.x.

848 IPCC. 2022. *Impacts, Adaptation, and Vulnerability. Working Group II Contribution to the IPCC Sixth*
849 *Assessment Report of the Intergovernmental Panel on Climate Change.*

850 Jorda, H., M.A. Ahmed, M. Javaux, A. Carminati, P. Duddek, et al. 2022. Field scale plant water relation of
851 maize (*Zea mays*) under drought – impact of root hairs and soil texture. *Plant Soil* 478(1–2): 59–84.
852 doi: 10.1007/s11104-022-05685-x.

853 Klein, T. 2014. The variability of stomatal sensitivity to leaf water potential across tree species indicates a
854 continuum between isohydric and anisohydric behaviours. *Funct. Ecol.*: 1313–1320. doi:
855 10.1111/1365-2435.12289.

856 Koehler, T., D.S. Moser, Á. Botezatu, T. Murugesan, S. Kaliamoorthy, et al. 2022. Going underground: soil
857 hydraulic properties impacting maize responsiveness to water deficit. *Plant Soil* 478(1–2): 43–58. doi:
858 10.1007/s11104-022-05656-2.

859 [Lärm, L., F.M. Bauer, N. Hermes, J. van der Kruk, H. Vereecken, et al. 2023. Multi-year belowground data
860 of minirhizotron facilities in Selhausen. *Sci. Data* 10\(1\): 1–15. doi: 10.1038/s41597-023-02570-9.](#)

861 Li, X., T.R. Sinclair, and L. Bagherzadi. 2016. Hydraulic Conductivity Changes in Soybean Plant–Soil System
862 with Decreasing Soil Volumetric Water Content. *J. Crop Improv.* 30(6): 713–723. doi:
863 10.1080/15427528.2016.1231729.

864 Li, Y., J.S. Sperry, and M. Shao. 2009. Hydraulic conductance and vulnerability to cavitation in corn (*Zea*
865 *mays* L.) hybrids of differing drought resistance. *Environ. Exp. Bot.* 66(2): 341–346. doi:
866 10.1016/j.envexpbot.2009.02.001.

867 Marin, M., D.S. Feeney, L.K. Brown, M. Naveed, S. Ruiz, et al. 2021. Significance of root hairs for plant
868 performance under contrasting field conditions and water deficit. *Ann. Bot.* 128(1): 1–16. doi:
869 10.1093/aob/mcaa181.

870 Meunier, F., A. Heymans, X. Draye, V. Couvreur, M. Javaux, et al. 2020. MARSHAL, a novel tool for virtual
871 phenotyping of maize root system hydraulic architectures. *In Silico Plants* 2(1): 1–15. doi:
872 10.1093/insilicoplants/diz012.

873 Meunier, F., M. Zarebanadkouki, M.A. Ahmed, A. Carminati, V. Couvreur, et al. 2018. Hydraulic
874 conductivity of soil-grown lupine and maize unbranched roots and maize root-shoot junctions. *J.*
875 *Plant Physiol.* 227(February): 31–44. doi: 10.1016/j.jplph.2017.12.019.

876 Morandage, S., J. Vanderborght, M. Zörner, G. Cai, D. Leitner, et al. 2021. Root architecture development

877 in stony soils. *Vadose Zo. J.* (April): 1–17. doi: 10.1002/vzj2.20133.

878 Müllers, Y., J.A. Postma, H. Poorter, and D. van Dusschoten. 2022. Stomatal conductance tracks soil-to-leaf
879 hydraulic conductance in faba bean and maize during soil drying. *Plant Physiol.* doi:
880 10.1093/plphys/kiac422.

881 Nguyen, T.H., M. Langensiepen, T. Gaiser, H. Webber, H. Ahrends, et al. 2022a. Responses of winter wheat
882 and maize to varying soil moisture: From leaf to canopy. *Agric. For. Meteorol.* 314(December 2021):
883 108803. doi: 10.1016/j.agrformet.2021.108803.

884 Nguyen, T.H., M. Langensiepen, H. Hueging, T. Gaiser, S.J. Seidel, et al. 2022b. Expansion and evaluation
885 of two coupled root–shoot models in simulating CO₂ and H₂O fluxes and growth of maize. *Vadose*
886 *Zo. J.* 21(3): 1–31. doi: 10.1002/vzj2.20181.

887 Nguyen, T.H., M. Langensiepen, J. Vanderborgh, H. Hüging, C.M. Mboh, et al. 2020. Comparison of root
888 water uptake models in simulating CO₂ and H₂O fluxes and growth of wheat. *Hydrol. Earth Syst. Sci.*
889 (24): 4943–4969. doi: 10.5194/hess-24-4943-2020.

890 Ordóñez, R.A., S. V. Archontoulis, R. Martinez-Feria, J.L. Hatfield, E.E. Wright, et al. 2020. Root to shoot
891 and carbon to nitrogen ratios of maize and soybean crops in the US Midwest. *Eur. J. Agron.* 120(June):
892 126130. doi: 10.1016/j.eja.2020.126130.

893 Passioura, J.B., 2006. The perils of pot experiments. *Funct. Plant Biol.* 33 (12), 1075–1079.
894 <https://doi.org/10.1071/FP06223>.

895 Ranawana SRWMCJK, Siddique KHM, Palta JA et al (2021) Stomata coordinate with plant hydraulics to
896 regulate transpiration response to vapour pressure deficit in wheat. *Functional Plant Biol* 48:839–850.
897 <https://doi.org/10.1071/FP20392>

898 Richards, R.A., G.J. Rebetzke, A.G. Condon, and A.F. van Herwaarden. 2002. Breeding Opportunities for
899 Increasing the Efficiency of Water Use and Crop Yield in Temperate Cereals. *Crop Sci.* 42(1): 111–
900 121. doi: 10.2135/cropsci2002.1110.

901 Rodriguez-Dominguez, C.M., and T.J. Brodribb. 2019. Declining root water transport drives stomatal
902 closure in olive under. *New Phytol.* 225: 126–134.

903 Sinclair, T.R., and M.M. Ludlow. 1986. Influence of soil water supply on the plant water balance of four
904 tropical grain legumes. *Aust. J. Plant Physiol.* 13: 329–341.

905 Scharwies, J.D., and J.R. Dinneny. 2019. Water transport, perception, and response in plants. *J. Plant Res.*
906 132(3): 311–324. doi: 10.1007/s10265-019-01089-8.

907 Schultz, H.R. 2003. Differences in hydraulic architecture account for near-isohydric and anisohydric
908 behaviour of two field-grown *Vitis vinifera* L. cultivars during drought. *Plant, Cell Environ.* 26(8):
909 1393–1405. doi: 10.1046/j.1365-3040.2003.01064.x.

910 Stadler, A., S. Rudolph, M. Kupisch, M. Langensiepen, J. van der Kruk, et al. 2015. Quantifying the effects
911 of soil variability on crop growth using apparent soil electrical conductivity measurements. *Eur. J.*
912 *Agron.* 64: 8–20. doi: 10.1016/j.eja.2014.12.004.

913 Sulis, M., V. Couvreur, J. Keune, G. Cai, I. Trebs, et al. 2019. Incorporating a root water uptake model based
914 on the hydraulic architecture approach in terrestrial systems simulations. *Agric. For. Meteorol.* 269–
915 270: 28–45. doi: <https://doi.org/10.1016/j.agrformet.2019.01.034>.

916 Sunita, C., T.R. Sinclair, C.D. Messina, and M. Cooper. 2014. Hydraulic conductance of maize hybrids

917 differing in transpiration response to vapor pressure deficit. *Crop Sci.* 54(3): 1147–1152. doi:
918 10.2135/cropsci2013.05.0303.

919 Tardieu, F., X. Draye, and M. Javaux. 2017. Root Water Uptake and Ideotypes of the Root System: Whole-
920 Plant Controls Matter. *Vadose Zo. J.* 16(9): 0. doi: 10.2136/vzj2017.05.0107.

921 Tardieu, F., and T. Simonneau. 1998. Variability among species of stomatal control under fluctuating soil
922 water status and evaporative demand: modelling isohydric and anisohydric behaviours. *J. Exp. Bot.*
923 49(March): 419–432. doi: 10.1093/jxb/49.Special_Issue.419.

924 Tardieu, F. 2016. Too many partners in root – shoot signals . Does hydraulics qualify as the only signal
925 that feeds back over time for reliable stomatal. *New Phytol.* 212: 802–804.

926 Trillo, N., and R.J. Fernández. 2005. Wheat plant hydraulic properties under prolonged experimental
927 drought: Stronger decline in root-system conductance than in leaf area. *Plant Soil* 277(1–2): 277–
928 284. doi: 10.1007/s11104-005-7493-5.

929 Tsuda, M., and M.T. Tyree. 1997. Whole-plant hydraulic resistance and vulnerability segmentation in
930 *Acer saccharinum*. *Tree Physiol.* (17): 351–357.

931 Turner, N.C., E.D. Schulze, and T. Gollan. 1984. The responses of stomata and leaf gas exchange to vapour
932 pressure deficits and soil water content - I. Species comparisons at high soil water contents.
933 *Oecologia* 63(3): 338–342. doi: 10.1007/BF00390662.

934 Tyree, M.T., E.L. Fiscus, S.D. Wullschleger, and M.A. Dixon. 1986. Detection of Xylem Cavitation in Corn
935 under Field Conditions. *Plant Physiol.* 82(2): 597–599. doi: 10.1104/pp.82.2.597.

936 Vadez, V. 2014. Root hydraulics : The forgotten side of roots in drought adaptation. *F. Crop. Res.* 165: 15–
937 24.

938 Vadez, V., S. Choudhary, J. Kholová, C.T. Hash, R. Srivastava, et al. 2021. Transpiration efficiency: Insights
939 from comparisons of C4cereal species. *J. Exp. Bot.* 72(14): 5221–5234. doi: 10.1093/jxb/erab251.

940 Vanderborght, J., V. Couvreur, F. Meunier, A. Schnepf, H. Vereecken, et al. 2021. From hydraulic root
941 architecture models to macroscopic representations of root hydraulics in soil water flow and land
942 surface models. *Hydrol. Earth Syst. Sci.* 25(9): 4835–4860. doi: 10.5194/hess-25-4835-2021.

943 Vanderborght, J., A. Graf, C. Steenpass, B. Scharnagl, N. Prolingheuer, et al. 2010. Within-Field Variability
944 of Bare Soil Evapora Θ on Derived from Eddy Covariance Measurements. *Vadose Zo. J.* 9: 943–954.
945 doi: 10.2136/vzj2009.0159.

946 Vereecken, H., A. Schnepf, J.W. Hopmans, M. Javaux, D. Or, et al. 2016. Modeling Soil Processes: Review,
947 Key Challenges, and New Perspectives. *Vadose Zo. J.* 15(5): vzj2015.09.0131. doi:
948 10.2136/vzj2015.09.0131.

949 Vetterlein, D., M. Phalempin, E. Lippold, S. Schlüter, S. Schreiter, et al. 2022. Root hairs matter at field
950 scale for maize shoot growth and nutrient uptake, but root trait plasticity is primarily triggered by
951 texture and drought. *Plant Soil* 478(1–2): 119–141. doi: 10.1007/s11104-022-05434-0.

952 Vitale, L., P. Di Tommasi, C. Arena, A. Fierro, A. Virzo De Santo, et al. 2007. Effects of water stress on gas
953 exchange of field grown *Zea mays* L. in Southern Italy: An analysis at canopy and leaf level. *Acta*
954 *Physiol. Plant.* 29(4): 317–326. doi: 10.1007/s11738-007-0041-6.

955 Wang, N., J. Gao, and S. Zhang. 2017. Overcompensation or limitation to photosynthesis and root hydraulic
956 conductance altered by rehydration in seedlings of sorghum and maize. *Crop J.* 5(4): 337–344. doi:

Formatted: German (Germany)

957 10.1016/j.cj.2017.01.005.

958 [Weihermüller, L., Huisman, J. A., Lambot, S., Herbst, M., & Vereecken, H. \(2007\). Mapping the spatial](#)
959 [variation of soil water content at the field scale with different ground penetrating radar techniques.](#)
960 [Journal of Hydrology, 340, 205–216. https://doi.org/10.1016/j.jhydrol.2007.04.013](#)

961 Welcker, C., W. Sadok, G. Dignat, M. Renault, S. Salvi, et al. 2011. A common genetic determinism for
962 sensitivities to soil water deficit and evaporative demand: Meta-analysis of quantitative trait loci and
963 introgression lines of maize. *Plant Physiol.* 157(2): 718–729. doi: 10.1104/pp.111.176479.

964 Zhuang, J., Y. Jin, and T. Miyazaki. 2001. ESTIMATING WATER RETENTION CHARACTERISTIC FROM SOIL
965 PARTICLE-SIZE DISTRIBUTION USING A NON-SIMILAR MEDIA CONCEPT. *Soil Sci.* 166(5).
966 [https://journals.lww.com/soilsci/Fulltext/2001/05000/ESTIMATING_WATER_RETENTION_CHARACT](https://journals.lww.com/soilsci/Fulltext/2001/05000/ESTIMATING_WATER_RETENTION_CHARACTERISTIC_FROM.2.aspx)
967 [ERISTIC_FROM.2.aspx.](https://journals.lww.com/soilsci/Fulltext/2001/05000/ESTIMATING_WATER_RETENTION_CHARACTERISTIC_FROM.2.aspx)

968 Zwieniecki, M.A., P.J. Melcher, C.K. Boyce, L. Sack, and N.M. Holbrook. 2002. Hydraulic architecture of leaf
969 venation in *Laurus nobilis* L. *Plant, Cell Environ.* 25(11): 1445–1450. doi: 10.1046/j.1365-
970 3040.2002.00922.x.

971

972

973

974

975

976

977

978

979

980

981

982

983

984

985

986 **Author contribution**

987 Huu Thuy Nguyen, Thomas Gaiser, Jan Vanderborght, and Frank Ewert: Conceptualization; Huu Thuy
988 Nguyen, and Hubert Hüging: Data curation and data quality check (aboveground measurements); Lena
989 Lärm, Felix Bauer, Anja Klotzsche, Jan Vanderborght, and Andrea Schnepf: data curation and data quality
990 check (belowground measurements); Huu Thuy Nguyen: Formal data analysis and visualization; Thomas
991 Gaiser, Jan Vanderborght, Andrea Schnepf, and Frank Ewert: Funding acquisition & Project administration;
992 Huu Thuy Nguyen: writing – original draft; all authors: review, editing, and finalizing the manuscript.

993 **Competing interests**

994 This manuscript has not been published and is not under consideration for publication in any other journal.
995 All authors agreed and approved the manuscript and its submission to this journal. We declare there is no
996 conflict of interest.

997 **Code/Data availability**

998 The meteorological data were collected from a weather station in Selhausen (Germany) which belongs to
999 the TERENO network of terrestrial observatories. Weather data are freely available from the TERENO data
1000 portal (<https://www.tereno.net/ddp/dispatch?searchparams=freetext-Selhausen>, last
1001 October 2020) (TERENO, 2020). The data which were obtained from the minirhizotron facilities (under-
1002 and aboveground) are available from the corresponding author on reasonable requests.

1003

1004

List of Figures

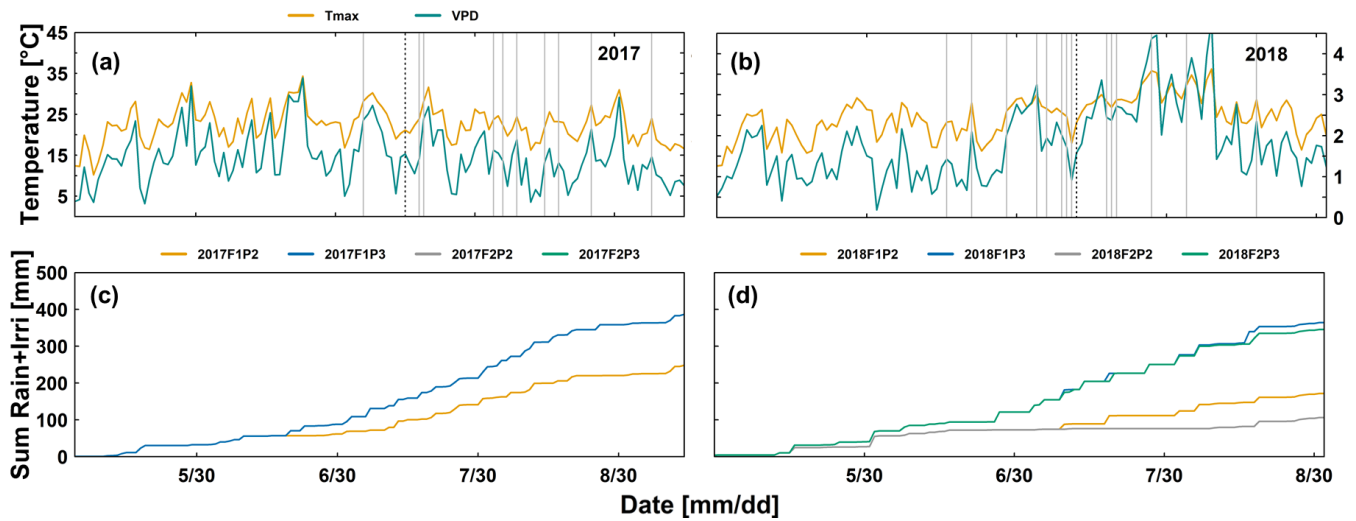


Figure 1: Daily maximum air temperature (Tmax) (°C), daily maximum air vapor pressure deficit (VPD) (kPa) in the two growing seasons (a) 2017 and (b) 2018 and cumulative (sum) of rainfall and irrigation from the rainfed (P2) and irrigated (P3) plots of the stony soil (F1) and silty soil (F2) in the two growing seasons (c) 2017 and (d) 2018. The black dashed vertical lines (a) and (b) indicate silking time. Grey vertical lines in (a) and (b) indicate the measured days for leaf gas exchange and leaf water potential. Two lines for 2017F2P2 and 2017F2P3 were overlapped by the lines from 2017F1P2 and 2017F1P3, respectively

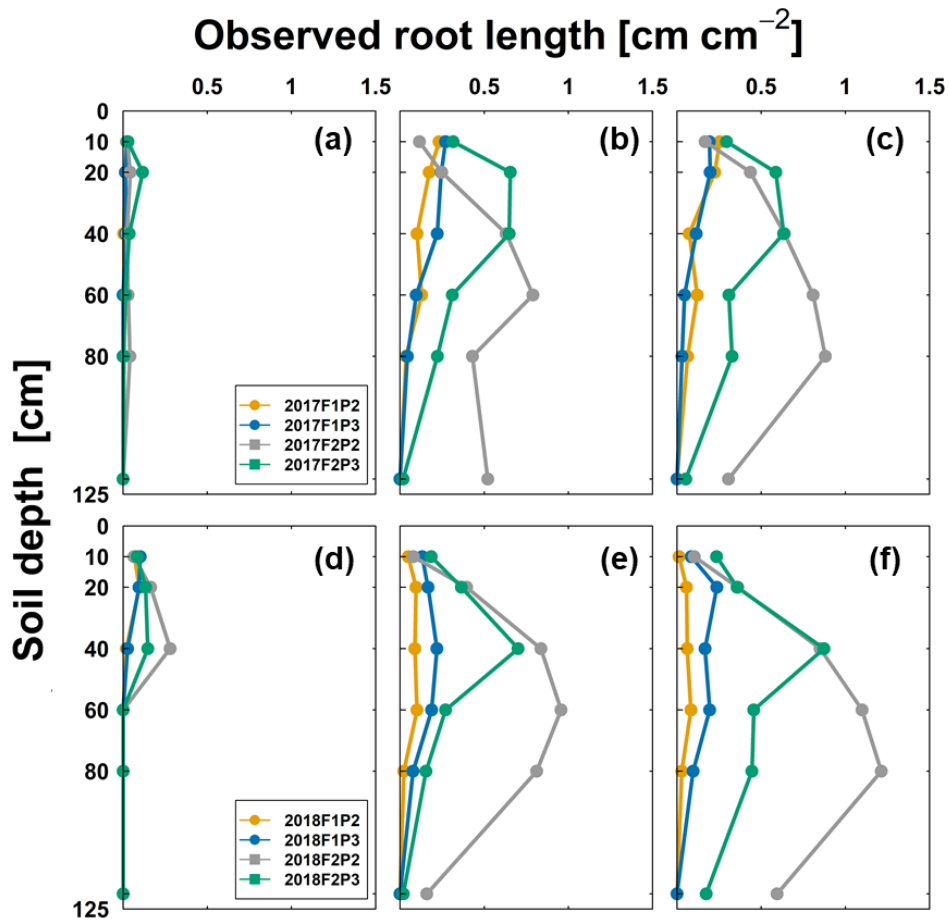


Figure 2: Observed root length from minirhizotubes (cm cm^{-2}) from 10, 20, 40, 60, 80, and 120 cm soil depth from the rainfed (P2) and irrigated (P3) plots of the stony soil (F1) and silty soil (F2) in the two growing seasons in 2017 (a - 8 June, b - at silking on 13 July, c - at harvest on 12 September) and in 2018 (d - 7 June, e - at one week after silking - 18 July, f - one week before harvest - 16 August).

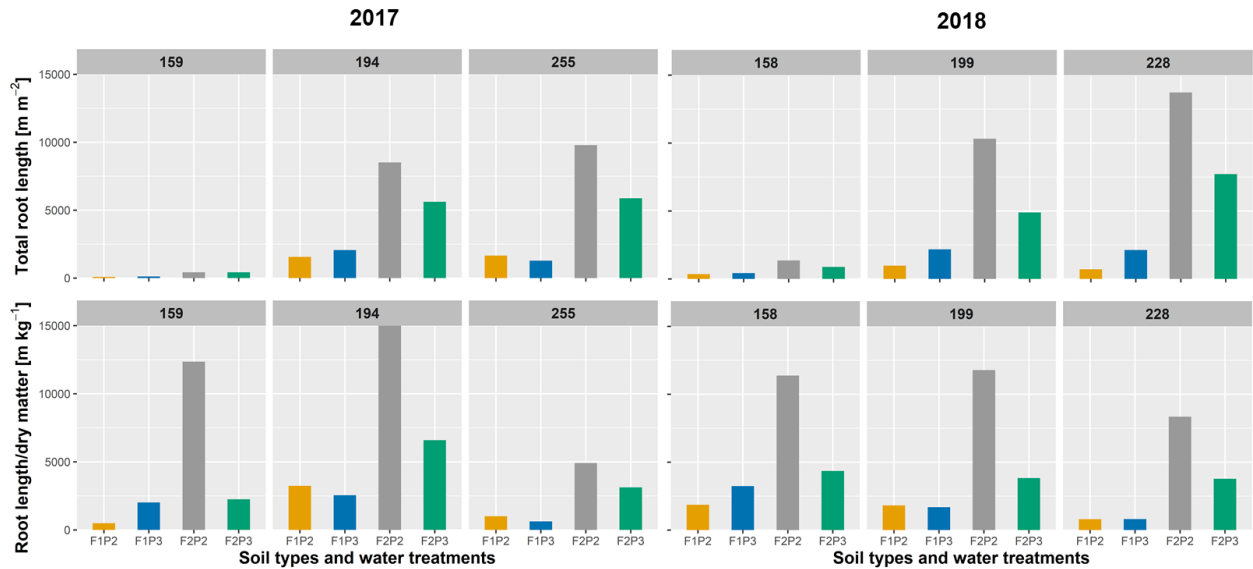


Figure 3: Observed root length from minirhizotubes (m m^{-2}) and ratio of root length per shoot dry matter (m kg^{-1}) from the rainfed (P2) and irrigated (P3) plots of the stony soil (F1) and silty soil (F2) in the two growing seasons (DOY 159, 194, and 255, left panel) in 2017 and in 2018 (DOY 158, 199, and 228, right panel) where on 8 June (DOY 159) at silking on 13 July (DOY194) 2017; and at harvest on 12 September (DOY 255) in 2017; 7 June (DOY 158), one week after silking on 18 July (DOY 199); and one week before harvest on 16 August (DOY 228) in 2018 (see also Figure 2).

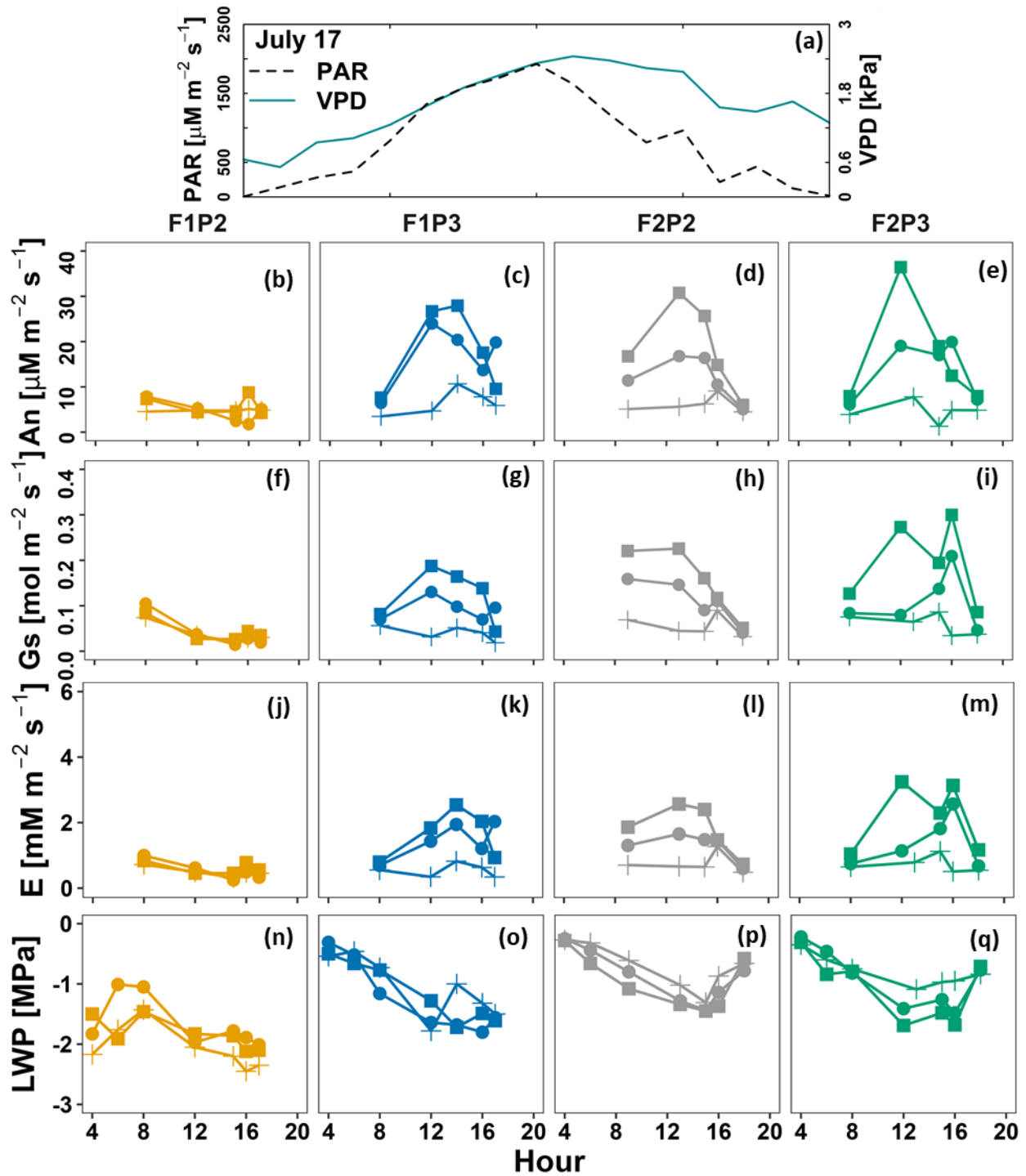


Figure 4. Diurnal course of (a) photosynthetically active radiation (PAR) and vapor pressure deficit (VPD), (b–e) leaf net photosynthesis (An), (f–i) leaf stomatal conductance (Gs), (j–m) leaf transpiration (E), and (n–q) leaf water potential (LWP) on 17 July in maize in 2018 before irrigation at the rainfed (P2) and irrigated (P3) plots of the stony soil (F1) and silty soil (F2). Measurement was carried out from shaded leaf (plus symbol with lines) and two sunlit leaves (solid dot - lines and solid square - lines).

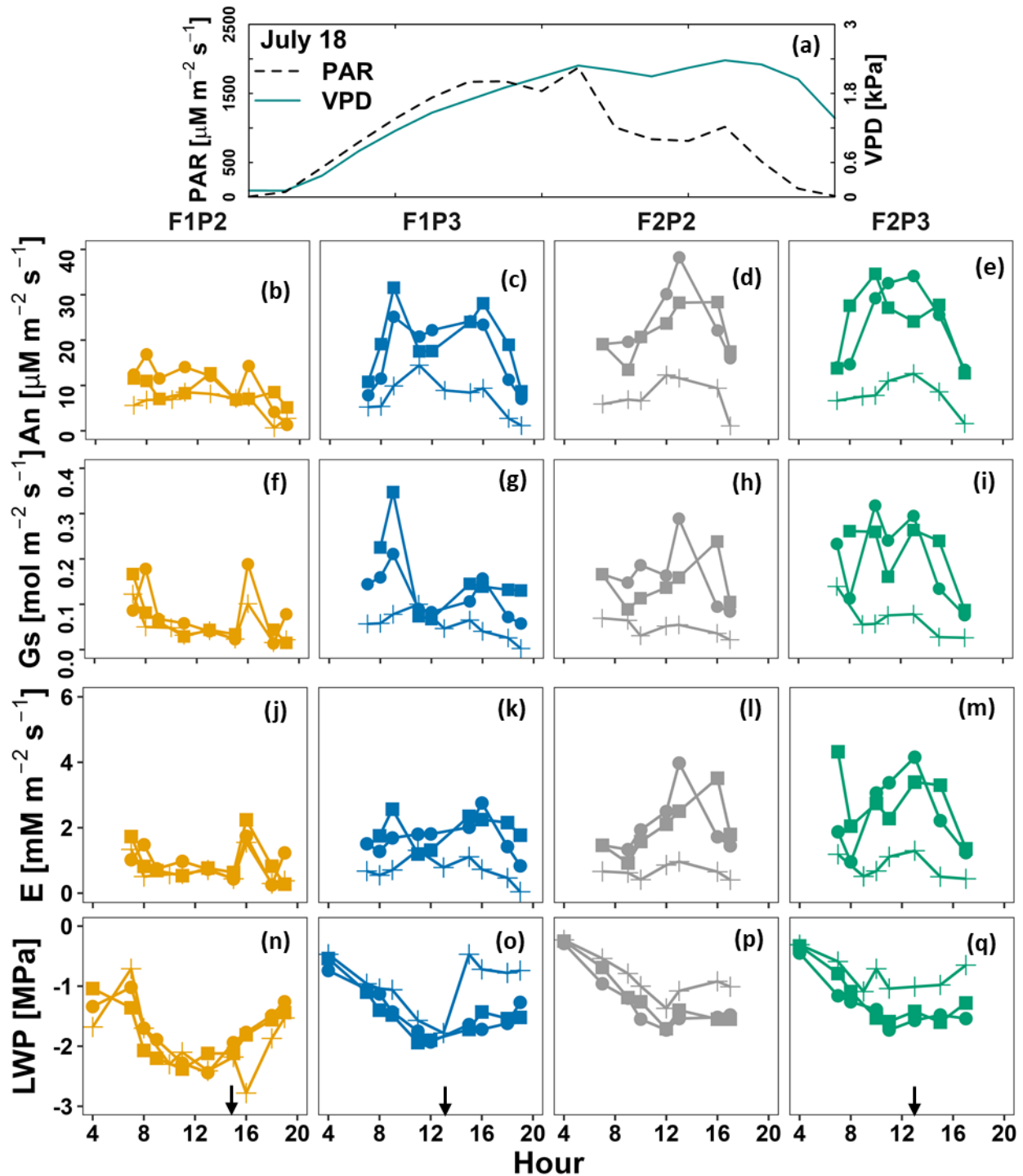


Figure 5. Diurnal course of (a) photosynthetically active radiation (PAR) and vapor pressure deficit (VPD), (b–e) leaf net photosynthesis (An), (f–i) leaf stomatal conductance (Gs), (j–m) leaf transpiration (E), and (n–q) leaf water potential (LWP) on 18 July in maize in 2018 before irrigation at the rainfed (P2) and irrigated (P3) plots of the stony soil (F1) and silty soil (F2). Measurement was carried out from shaded leaf (plus symbol with line) and two sunlit leaves (solid dot - lines and solid square - lines). Crop was irrigated at 1 PM, 1 PM, 4 PM for F1P3, F2P3, and F1P2, respectively (22.75 mm for each plot) (Supp. 2). **Black arrows indicate time of irrigation.**

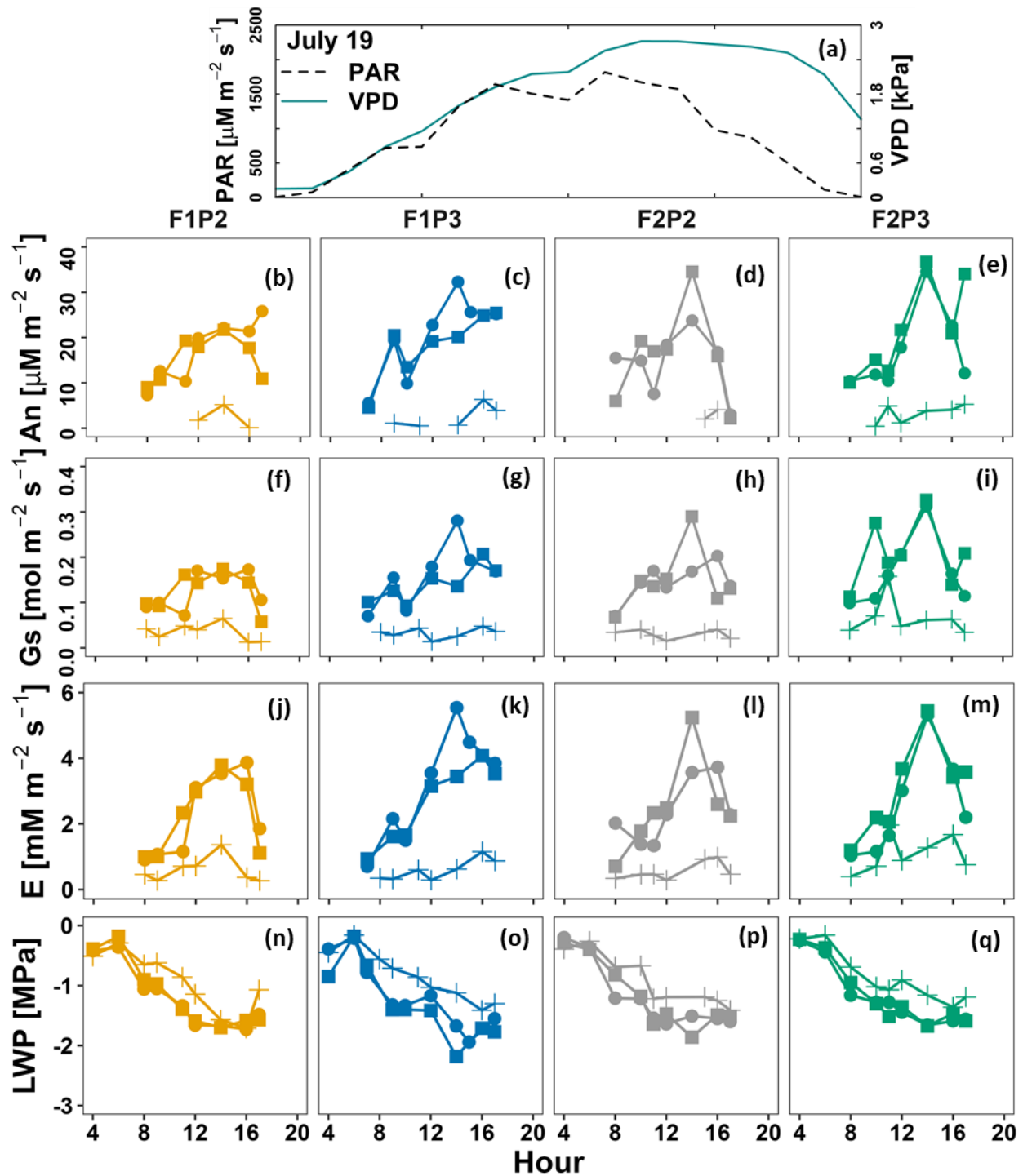


Figure 6. Diurnal course of (a) photosynthetically active radiation (PAR) and vapor pressure deficit (VPD), (b–e) leaf net photosynthesis (An), (f–i) leaf stomatal conductance (Gs), (j–m) leaf transpiration (E), and (n–q) leaf water potential (LWP) on 19 July in maize in 2018 after irrigation at the rainfed (P2) and irrigated (P3) plots of the stony soil (F1) and silty soil (F2). Measurement was carried out from shaded leaf (plus symbol with line) and two sunlit leaves (solid dot - lines and solid square -lines). Crop was irrigated on 18 July at 1 PM, 1 PM, 4 PM for F1P3, F2P3, and F1P2, respectively (22.75 mm for each plot) (Supp. 2).

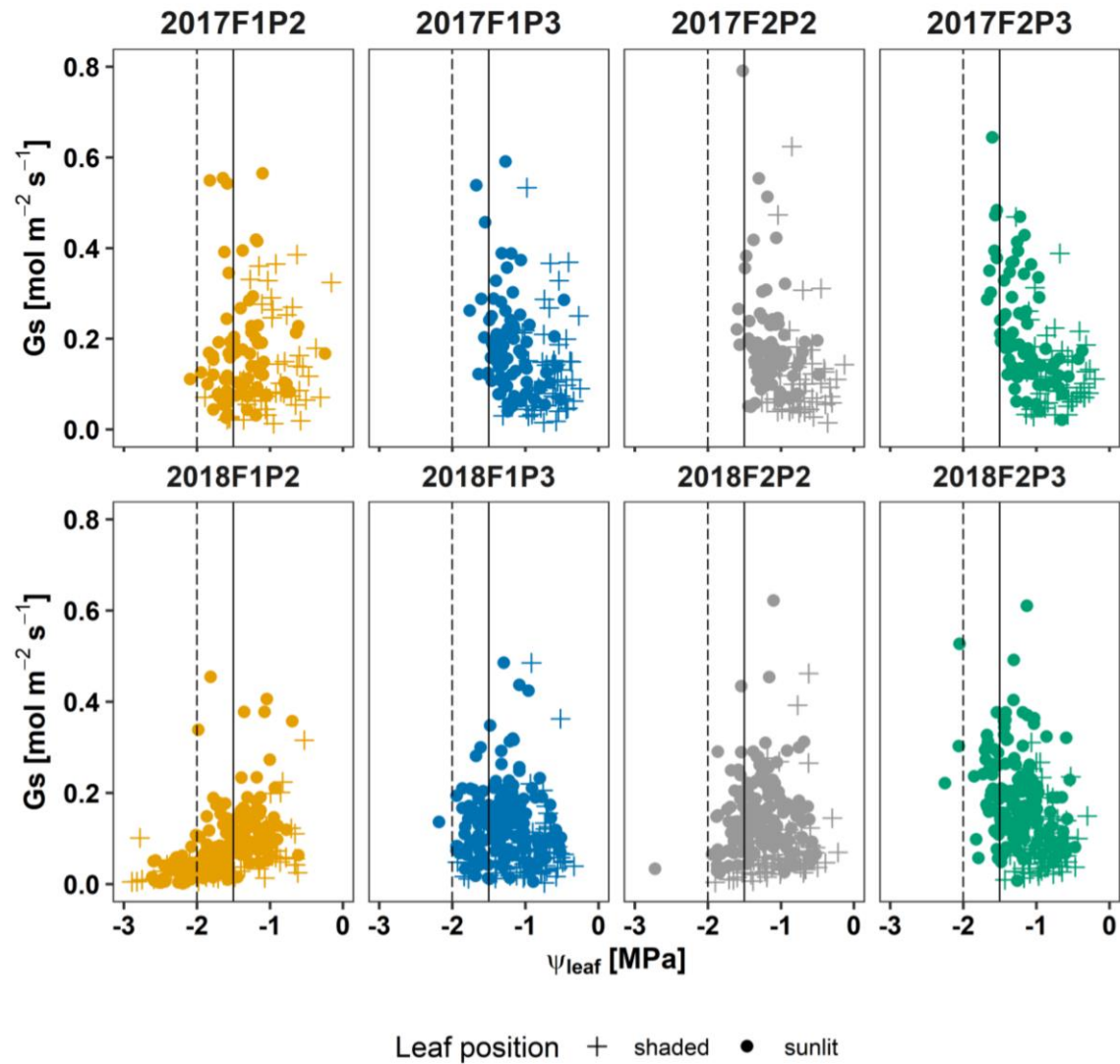


Figure 7: Seasonal stomatal conductance to water vapor (G_s) versus leaf water potential (ψ_{leaf}) in 2017 (top panel) and in 2018 (bottom panel) at the rainfed (P2) and irrigated (P3) plots of the stony soil (F1) and silty soil (F2). Vertically continuous and dashed lines indicated ψ_{leaf} at -1.5 and -2 MPa, respectively. Measurement was carried out from shaded leaf (plus symbol) and two sunlit leaves (solid dots)

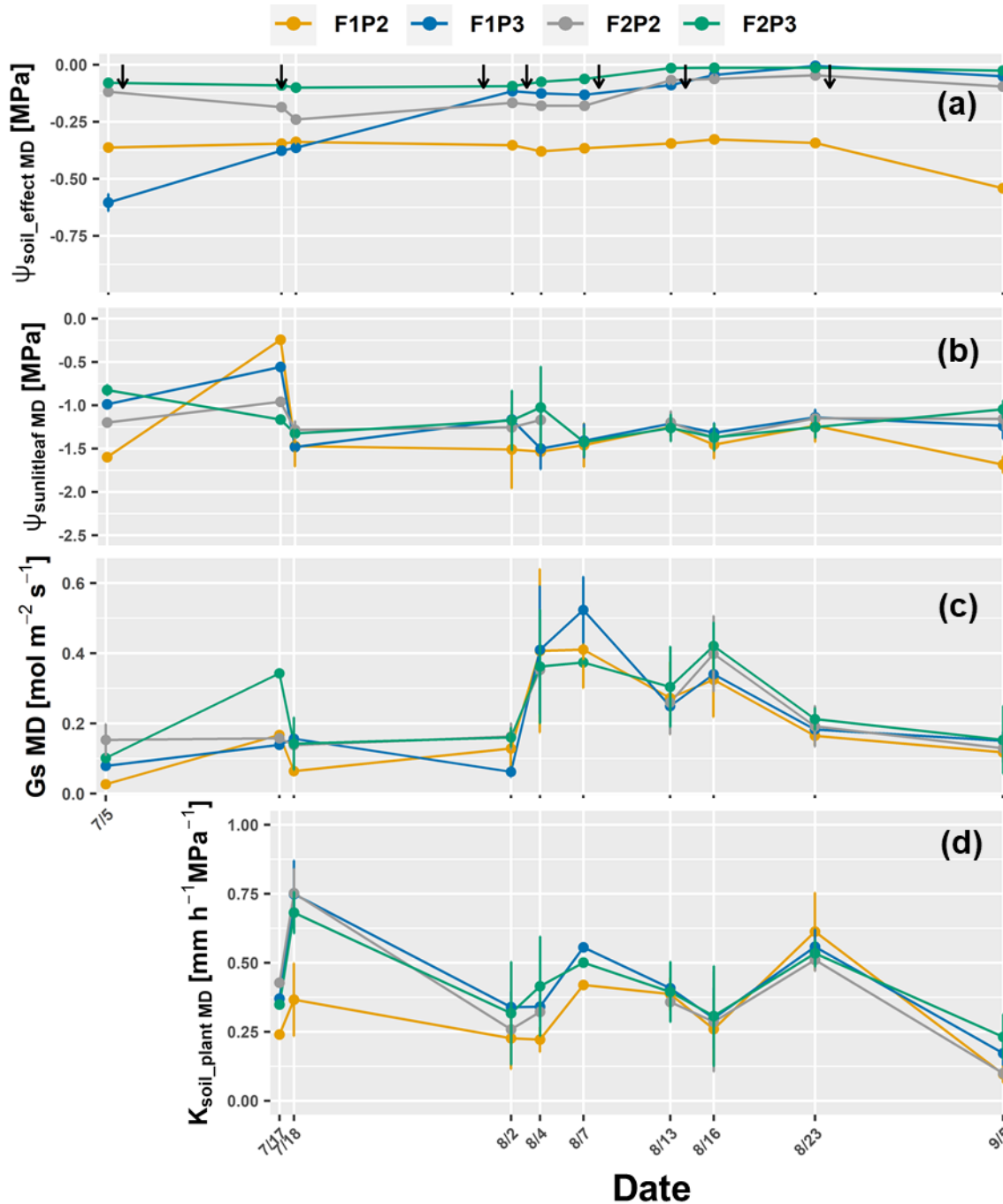


Figure 8: Dynamic of around midday (MD) of (a) the effective soil water potential ($\psi_{\text{soil_effec_MD}}$) (b) sunlit leaf water potential ($\psi_{\text{sunlitleaf_MD}}$), (c) stomatal conductance (Gs MD) and (d) whole soil-plant hydraulic conductance ($K_{\text{soil_plant_MD}}$) in the growing season 2017 from the rainfed (P2) and irrigated (P3) plots of the stony soil (F1) and silty soil (F2). Error bars indicate the standard deviation of the different values taken around midday (11 AM, 12AM, 1PM, and 2 PM) of different sunlit leaves. Whole soil-plant hydraulic conductance was shown from 17 July when sap flow was measured. The black arrows indicates the irrigation events for the irrigated treatments F1P3 and F2P3 in the showing period.

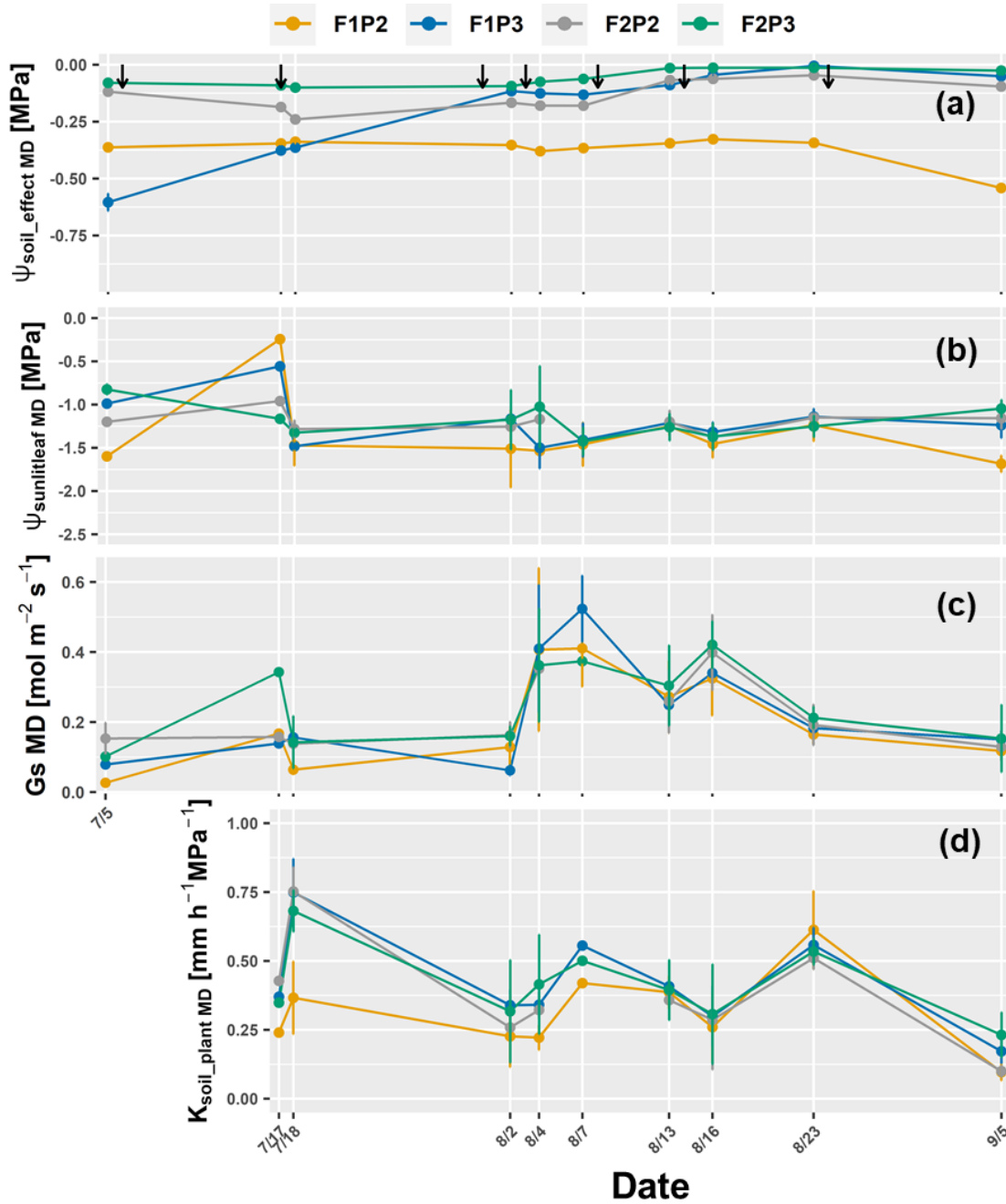


Figure 9: Dynamic of around midday (MD) of (a) the effective soil water potential ($\psi_{\text{soil_effec MD}}$) (b) sunlit leaf water potential ($\psi_{\text{sunlitleaf MD}}$), (c) stomatal conductance ($G_s \text{ MD}$) and (d) whole soil-plant hydraulic conductance ($K_{\text{soil_plant MD}}$) in the growing season 2018 from the rainfed (P2) and irrigated (P3) plots of the stony soil (F1) and silty soil (F2). Error bars indicate the standard deviation of the different values taken around midday (11 AM, 12AM, 1PM, and 2 PM) Leaf water potential and stomatal conductance were 2 sunlit leaves and one shaded leaf at each measured hour. Whole soil-plant hydraulic conductance was shown from 3 July when sap flow was measured. The black arrows indicates the irrigation events for the irrigated treatments F1P3 and F2P3 while the orange arrow indicates the irrigation application for the rainfed plot at the stony soil (F1P2).

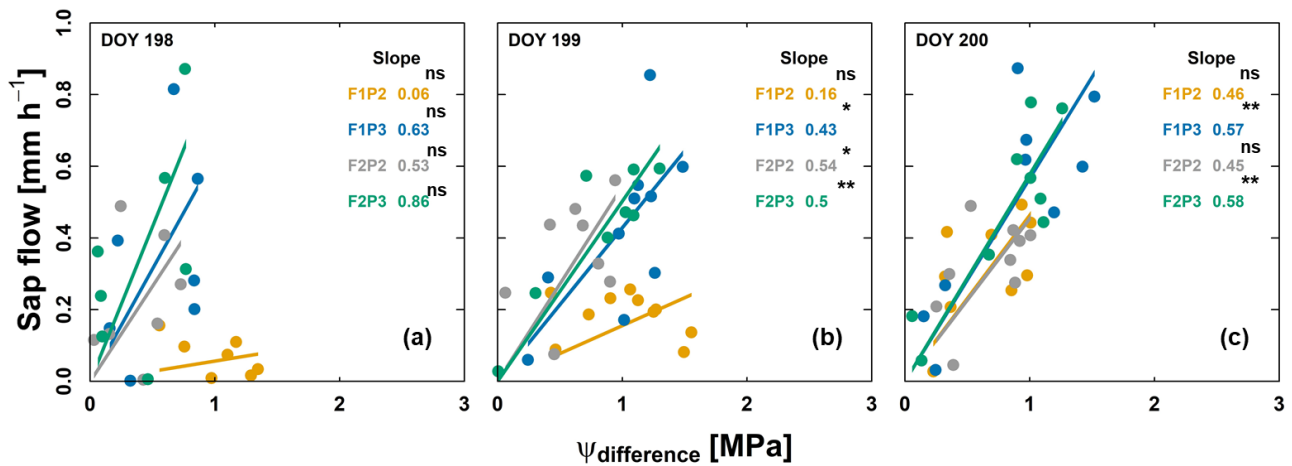


Figure 10: Relationship of sap flow and difference of effective soil water potential and sunlit leaf water potential ($\Psi_{\text{difference}}$) from the rainfed (P2) and irrigated (P3) plots of the stony soil (F1) and silty soil (F2) on three consecutive measurement days from predawn in 2018 (a) 17 July - DOY 198, (b) 18 July - DOY 199 and (c) 19 July - DOY 200. Crop was irrigated on 18 July (DOY 199) at 1 PM, 1 PM, and 4 PM for F1P3, F2P3, and F1P2, respectively (22.75 mm for each plot). The unit of slope in the linear regression (or soil-plant hydraulic conductance) is $\text{mm h}^{-1} \text{MPa}^{-1}$. Regression was based on the DEMING approach. The asterisk which are next to the slopes indicate a significant correlation between two variables according to Pearson method (ns: non-significant; * $p < 0.05$; ** $p < 0.01$; *** $p < 0.001$).

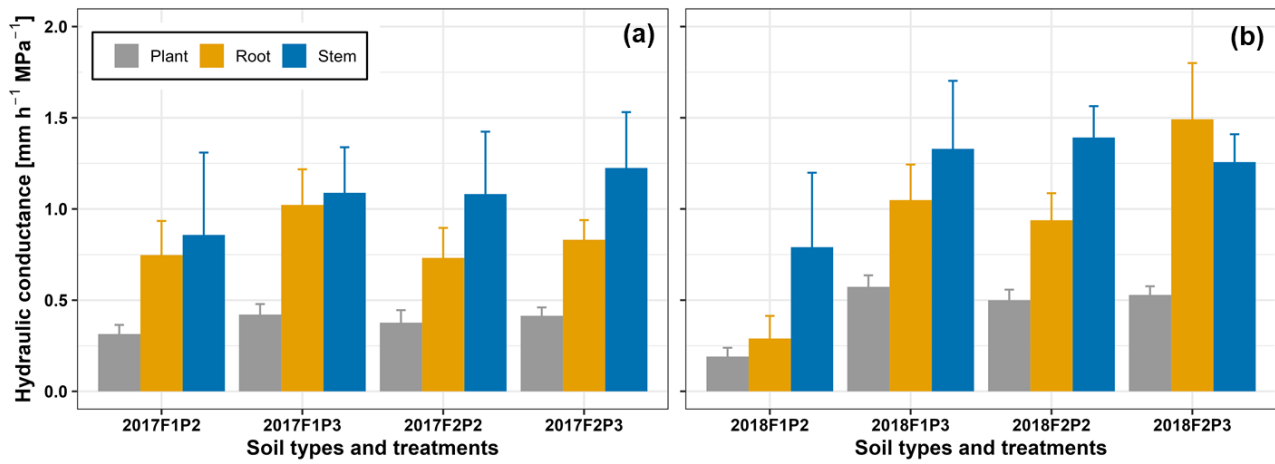


Figure 11: Comparison of different midday hydraulic components ($\text{mm h}^{-1} \text{MPa}^{-1}$): soil-plant (grey bars), soil-root (yellow bars), and stem (blue bars) from the rainfed (P2) and irrigated (P3) plots of the stony soil (F1) and silty soil (F2) in the two growing seasons (a) in 2017 and (b) in 2018. The error bars indicate the standard deviation from measurements around midday (11 AM, 12AM, 1PM, and 2 PM) in different measured days (in 2017 with $n = 4 \times 9$ days, Supplementary material 6, 7, and Fig. 8 and in 2018 with $n = 4 \times 10$ days, Supplementary material 6, 8, and Fig. 9).

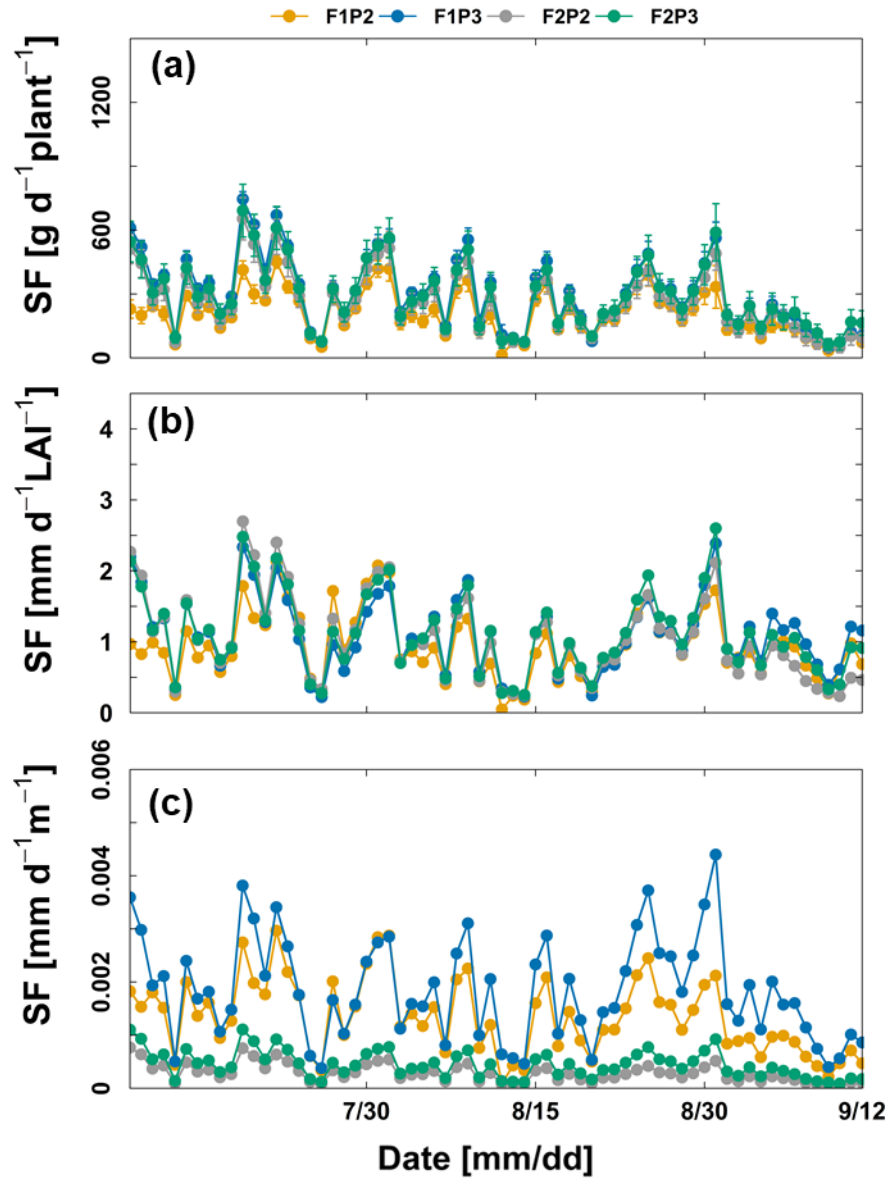


Figure 12: Comparison of sap flow (SF) in growing season 2017 from the rainfed (P2) and irrigated (P3) plots of the stony soil (F1) and silty soil (F2) with (a) sap flow per single plant (b) sap flow per leaf area index (LAI) and (c) sap flow per total root length. Data is shown from 9 July to 12 September 2017. Error bars in (a) indicate the standard deviation of the sap flow measurements in the five different maize plants.

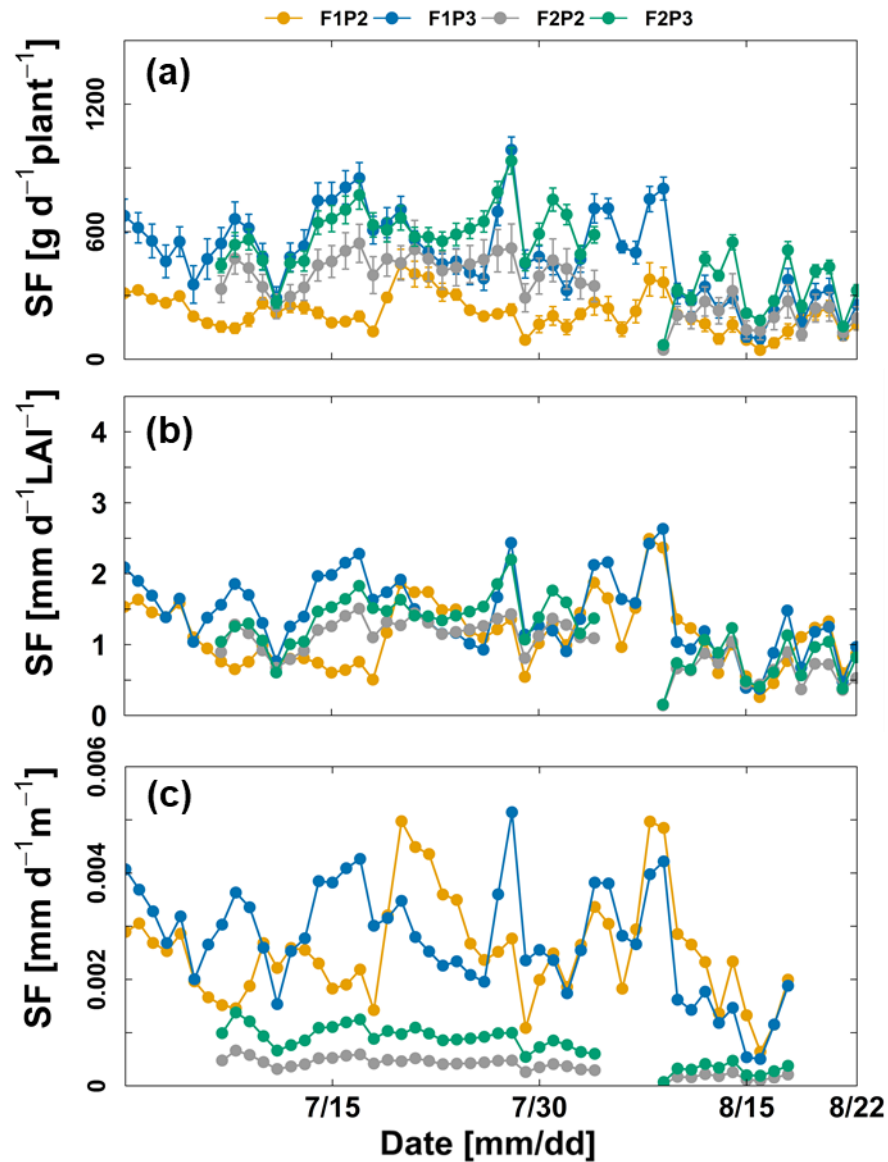


Figure 13: Comparison of sap flow (SF) in growing season 2018 from the rainfed (P2) and irrigated (P3) plots of the stony soil (F1) and silty soil (F2) with (a) sap flow per single plant (b) sap flow per leaf area index (LAI) and (c) sap flow per total root length. Data is shown in (a, b) from 29 June and 6 July for the stony soil (F1) and silty soil (F2), respectively to 21 August, 2018. Missing values of the beginning of the growing season and from 3 August to 6 August 2018 in the F2P2 and F2P3 were due to the missing values of measured sap flow because of sensor disconnection. Missing values in (c) at the end of the growing season in F2P2 and F2P3 was due to no availability of root measurement. Error bars in (a) indicate the standard deviation of the sap flow measurements in the five different maize plants.

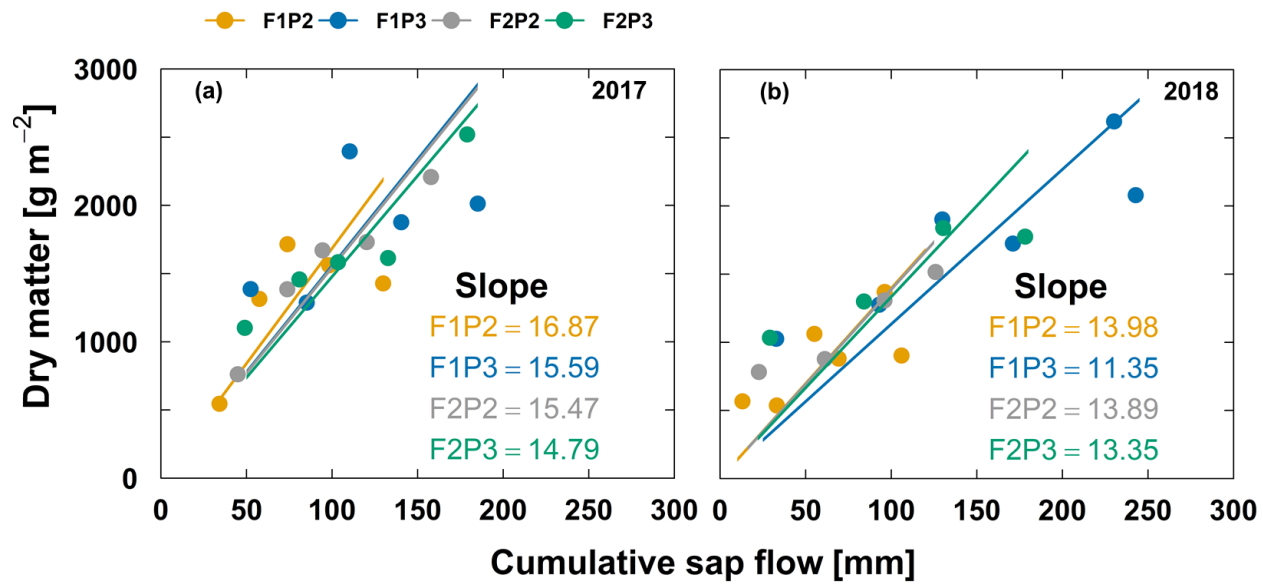


Figure 14: Relationship of aboveground dry matter and cumulative sap flow from the rainfed (P2) and irrigated (P3) plots of the stony soil (F1) and silty soil (F2) in the two growing seasons (a) 2017 and (b) 2018. The unit of slope linear relationship is g mm⁻¹. The less number of data points in (b) in 2018 from the F2P2 and F2P3 plots were due to the missing values of measured sap flow because of sensor disconnection. **For aboveground dry matter, each point represents the average of two sampling replicates, except the harvest with 5 sampling replicates.**